AD NUMBER

AD253633

LIMITATION CHANGES

TO:

Approved for public release; distribution is unlimited. Document partially illegible.

FROM:

**Distribution authorized to U.S. Gov't. agencies and their contractors;
Administrative/Operational Use; JAN 1961. Other requests shall be referred to Office of Naval Research, 875 North Randolph Street, Arlington VA 22203-1995. Document partially illegible.**

AUTHORITY

ONR ltr, 26 Oct 1977

AD 253 633

DISCLAIMER NOTICE

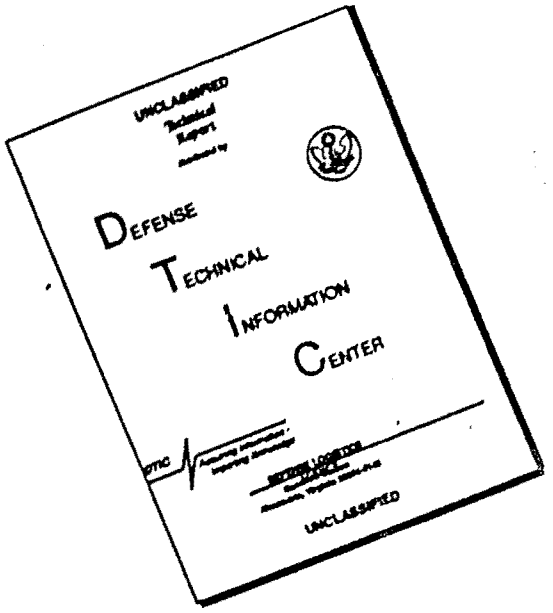

THIS DOCUMENT IS BEST QUALITY AVAILABLE. THE COPY FURNISHED TO DTIC CONTAINED A SIGNIFICANT NUMBER OF PAGES WHICH DO NOT REPRODUCE LEGIBLY.

Report Number

I-61-1

Effects of Injection Location on Combustion Instability in Premixed Gaseous Bipropellant Rocket Motors

by

J. R. Osborn and L. R. Davis

Interim Report No. 4

Contract N7 onr 39418

January 1961

JET PROPULSION CENTER
PURDUE UNIVERSITY

SCHOOL OF MECHANICAL ENGINEERING
LAFAYETTE, INDIANA

PURDUE UNIVERSITY

AND

PURDUE RESEARCH FOUNDATION

Lafayette, Indiana

Report No. I-61-1

EFFECTS OF INJECTION LOCATION ON COMBUSTION INSTABILITY IN PREMIXED GASEOUS BIPROPELLANT ROCKET MOTORS

by

J. R. Osborn and L. R. Davis

Interim Report No. 4

Contract N7 onr 39418

Jet Propulsion Center

Purdue University

January 1961

ACKNOWLEDGMENTS

The authors wish to thank Dr. M. J. Zucrow, Atkins Professor of Engineering, Purdue University, for his helpful guidance throughout the course of the investigation. The authors are also grateful to Messrs. W. H. Hennings and P. L. Nine for their helpful assistance in conducting part of the investigation, and to all other personnel of the Purdue Jet Propulsion Center.

Acknowledgment is also given to the Office of Naval Research, Contract N7 onr 39418 and the Air Force Office of Scientific Research, Contract AF 49(638)-756 under whose sponsorship the research reported herein was conducted. Reproduction in full or in part is permitted for any use of the United States Government.

TABLE OF CONTENTS

TABLE OF CONTENTS (Continued)

LIST OF FIGURES

LIST OF FIGURES (Continued)

LIST OF TABLES

ABSTRACT

The experiments reported herein were conducted for determining how basic injection variables influence high frequency combustion pressure oscillations in rocket motors. A gaseous bipropellant rocket motor burning ethylene and air as propellants was utilized. The three basic injection schemes included in the investigation were:

(1) injection at the head end of the motor,

(2) injection at the side of the combustion chamber, and

(3) injection at the nozzle end of the motor.

The experiments indicated that the injection location and pattern have a profound effect on the mode and occurrence of combustion pressure oscillations. It was determined that the mode of oscillation could be predicted by choosing the right injector. Furthermore, combustion oscillations could be completely suppressed by injecting at the proper location. This latter location was different for the different modes as would be expected.

INTRODUCTION

Stable combustion during the testing of a rocket motor is of prime importance for the successful operation of the motor. When combustion instability occurs in a rocket motor, the heat transfer rate to the combustion chamber walls greatly increases. Consequently, the walls rapidly reach excessive temperatures, and structural failure is usually the end result.

It has been found in the studies of high frequency oscillations (1) (2)* that injection plays a very important role in the instability of a rocket motor. The experiments reported herein were designed to study some of the basic injection variables and their effects on combustion instability in a rocket motor burning premixed gases. The injection schemes considered in this investigation are shown in Fig. 1.

The experiments conducted herein were divided into three phases:

Phase I — Investigation of the effects of injection from the head end of the motor on transverse combustion pressure oscillations.**

Phase II — Investigation of the effects of injection from the chamber walls on transverse and longitudinal combustion pressure oscillations.

Phase III — Investigation of the effects of injection from the nozzle end of the motor on transverse combustion pressure oscillations.

---

* Numbers in parentheses indicate references in the Bibliography.

** A discussion of the modes of combustion pressure oscillations is presented in Appendix B.

PHASE 1

HEAD END INJECTION

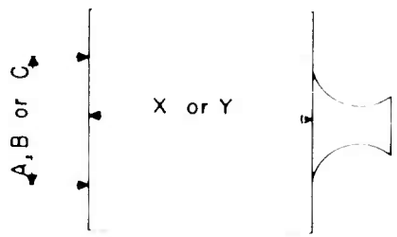

A= 6" INJECTION CIRCLE DIA.

B= 4" INJECTION CIRCLE DIA.

C= 2" INJECTION CIRCLE DIA.

X= 2" CHAMBER LENGTH

Y= 6" CHAMBER LENGTH

PHASE 2

SIDE INJECTION

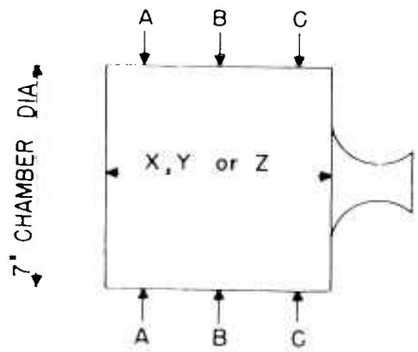

A= 1" FROM HEAD END

B= MID-POINT OF CHAMBER

C= 1" FROM NOZZLE

X= 2" CHAMBER LENGTH

Y= 6" CHAMBER LENGTH

Z= 14" CHAMBER LENGTH

PHASE 3

NOZZLE END INJECTION

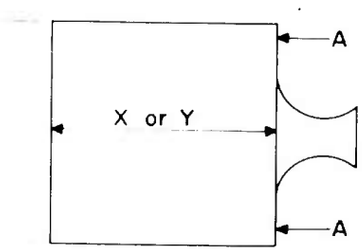

A= 6" INJECTION CIRCLE DIA.

X= 2" CHAMBER LENGTH

Y= 6" CHAMBER LENGTH

Fig. 1 Injection Schemes

Upon completion of this study the first phase of a long range combustion instability research program was completed. The complete program is described in References (3) and (4). The program is a logical sequence of steps starting with lower order combustion systems burning premixed gases to higher order systems burning unmixed liquids. Each progressive step adds one or more variables to the previous phase. The final goal is the combination of all phases to a useful conclusion which would help in the design of rocket motors free from combustion pressure oscillations.

A description of the previous experimental work done on high frequency combustion pressure oscillations performed at the Purdue Jet Propulsion Center is presented in References (3) through (8).

METHOD OF INVESTIGATION

General Discussion

A rocket motor having a 7 in. inside diameter and burning premixed ethylene and air was used in all of the experiments reported herein. The use of premixed gases eliminated such factors as vaporization, mixing, and atomization. Since only one fuel-oxidizer combination was burned, the only variable under investigation was that of the location of the injection of the unburned propellants. That is, the location of the heat release obtained from the combustion process. This location is important for determining both the mode and amplitude of the oscillations. Several locations of the injection of the unburned propellants were selected with a view toward determining whether or not the different modes could be excited. Those locations are discussed separately below.

Each rocket motor system discussed below was operated over an operating range from a mean chamber pressure of 20 psia to about 200 psia and from an equivalence ratio* below the lower inflammability limit to about 1.8 at 200 psia mean chamber pressure and to about 4.0 at lower mean chamber pressures. The upper limits to the operating range were subject to the limitations of the propellant supply systems.

---

* Equivalence ratio is defined as the fuel-air ratio by weight divided by the stoichiometric fuel-air ratio by weight.

Figure 2 illustrates the thrust stand and an experimental rocket motor equipped with side injection.

Any periodic combustion pressure oscillations that occurred during the operation of the motor were recorded on a multi-channel magnetic tape recorder. The propellant flow rates and mean chamber pressure at which the oscillations occurred were also recorded. The mode and amplitude of the pressure oscillations were determined from the pressure signals recorded by the tape recorder.

From the data obtained, the so-called instability regions (see Fig. 4 for a typical region) were determined thereby defining the stable and unstable operation of a given injection and combustion chamber system. A comparison of the instability regions, mode, and maximum amplitude of the pressure oscillations was made of the different injection schemes. Conclusions were then drawn concerning the effects of the various injection locations (heat release locations) on the several modes of combustion instability.

A description of the apparatus and the procedure for conducting each rocket motor run and evaluating the data from a run are presented in Appendices C and D respectively.

Experiments Employing Head End Injection

Three different injection patterns were employed to determine the effects of injection location in the head end of the combustion chamber on combustion instability. Figure 3 illustrates the three different patterns. A complete description of the head end injection system is given in Appendix C. Each injector was tested in 2 in. and 6 in. long combustion chambers over the previously mentioned ranges of mean chamber

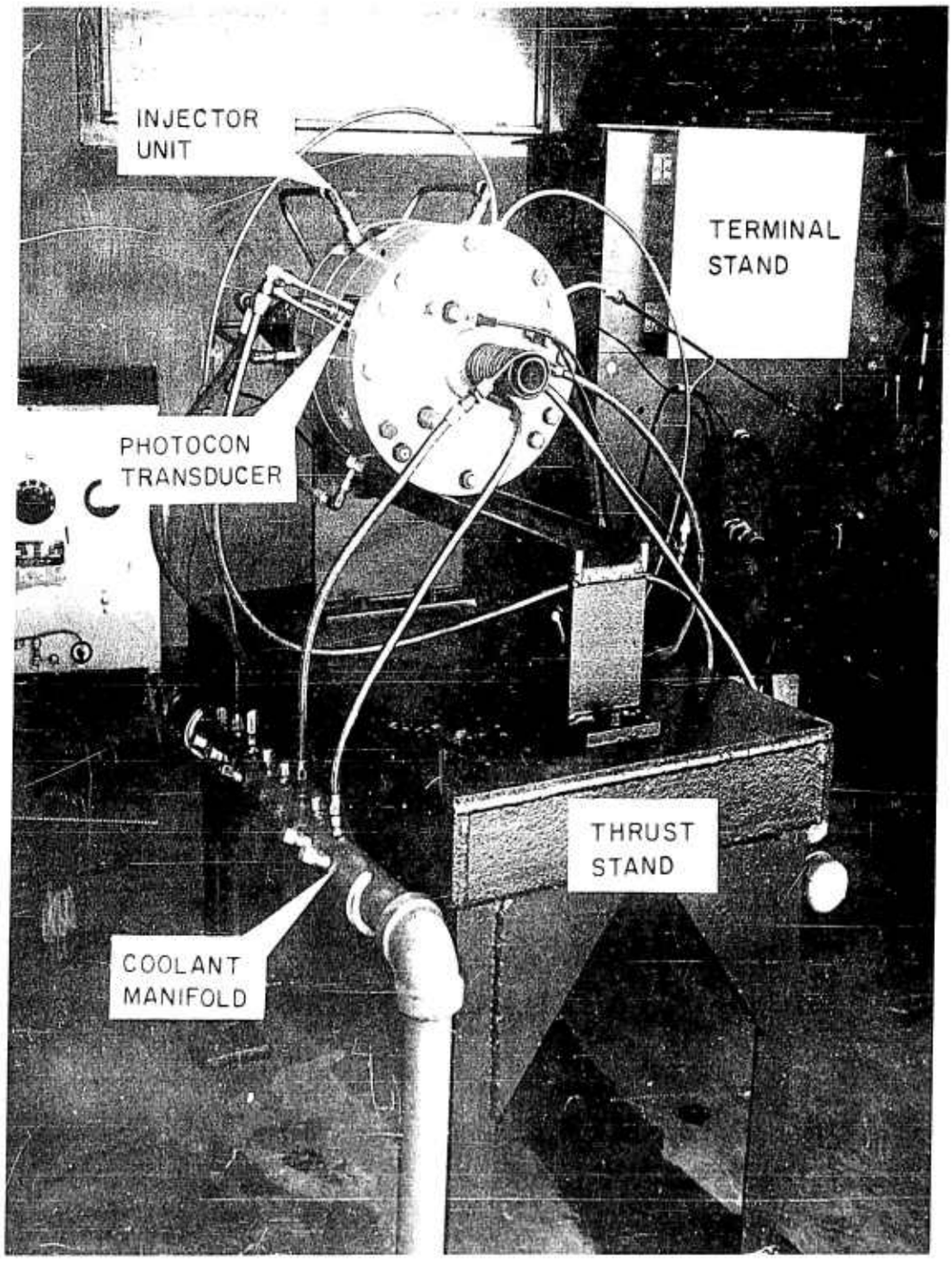

Fig. 2 Rocket Motor Installation

12 INJECTION HOLES, 0.177" DIA. — 7" CHAMBER DIAMETER

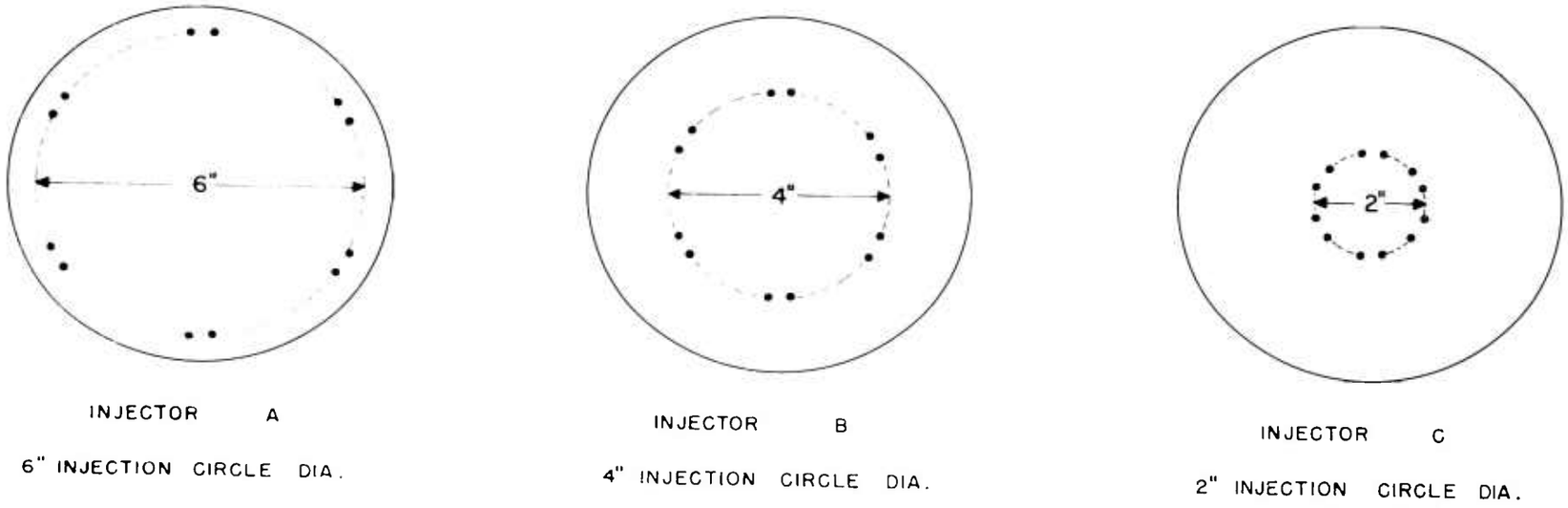

INJECTOR A

6" INJECTION CIRCLE DIA.

INJECTOR B

4" INJECTION CIRCLE DIA.

INJECTOR C

2" INJECTION CIRCLE DIA.

Fig. 3 Head End Injection Patterns

pressure and equivalence ratio. From the data obtained, the instability region, mode, and amplitude of the combustion pressure oscillations supported by each injection scheme was determined so that comparisons could be made to the other systems.

Experiments Employing Side Injection

Injection in the side of the chamber was accomplished with six individual injector units each containing two injection holes. Each unit was identical to a unit used in the head end injection system. The injector units were equally spaced around a 2 in. long combustion chamber spacer. By proper arrangement of the combustion chamber spacers, side injection could be accomplished at several different distances from the nozzle. A complete description of the side injection system is given in Appendix C.

The side injection systems were operated over the previously mentioned operating range with chamber lengths of 2, 6, and 14 inches. In the 6 and 14 in. chambers, the propellants were injected 1 in. from the head end of the chamber, 1 in. from the nozzle end of the chamber, and midway between the head end and nozzle end of the chamber. As for the case of the head end injection studies, the instability region, mode and amplitude of the combustion pressure oscillations were determined for each side injection scheme.

Experiments Employing Nozzle End Injection

The individual injector units used in the side end injection studies were employed in the nozzle end injection studies. The injector units were located in the nozzle plate so as to give the same injection pattern

as injector A in the head end injection studies (see Fig. 3).

The nozzle end injection system was operated with chamber lengths of 2 and 6 in. and the mean chamber pressures and equivalence ratios mentioned above. As in the previous phases, the instability region, mode, and amplitude of the pressure oscillations supported by nozzle injection were determined.

EXPERIMENTAL RESULTS

Instability Regions

Head End Injection

Instability regions are a graphical means of illustrating that portion of the total operating region of a particular motor where combustion pressure oscillations occur. Figure 4 is a typical instability region. The outer boundary divides the operating region of the motor into a region of steady or no combustion (outside the curve) and a region of oscillatory combustion (inside the curve). The lines inside the region represent lines of constant peak-to-peak amplitude of the pressure oscillations.

Figures 4 and 5 are the instability regions for head end injector A with injection holes on a 6 in. diameter circle. Figure 4 is for a 2 in. long chamber and Fig. 5 is for a 6 in. long chamber. The instability region for the 2 in. length is larger than that observed for the 6 in. length and the combustion oscillations occurred at a mean chamber pressure as low as 27 psia. A region of high amplitude (up to 80.0 psid) oscillations was found near the lower inflammability limit and another one near an equivalence ratio of 1.8. The instability region for the 6 in. long chamber is similar to the region found for the 2 in. long

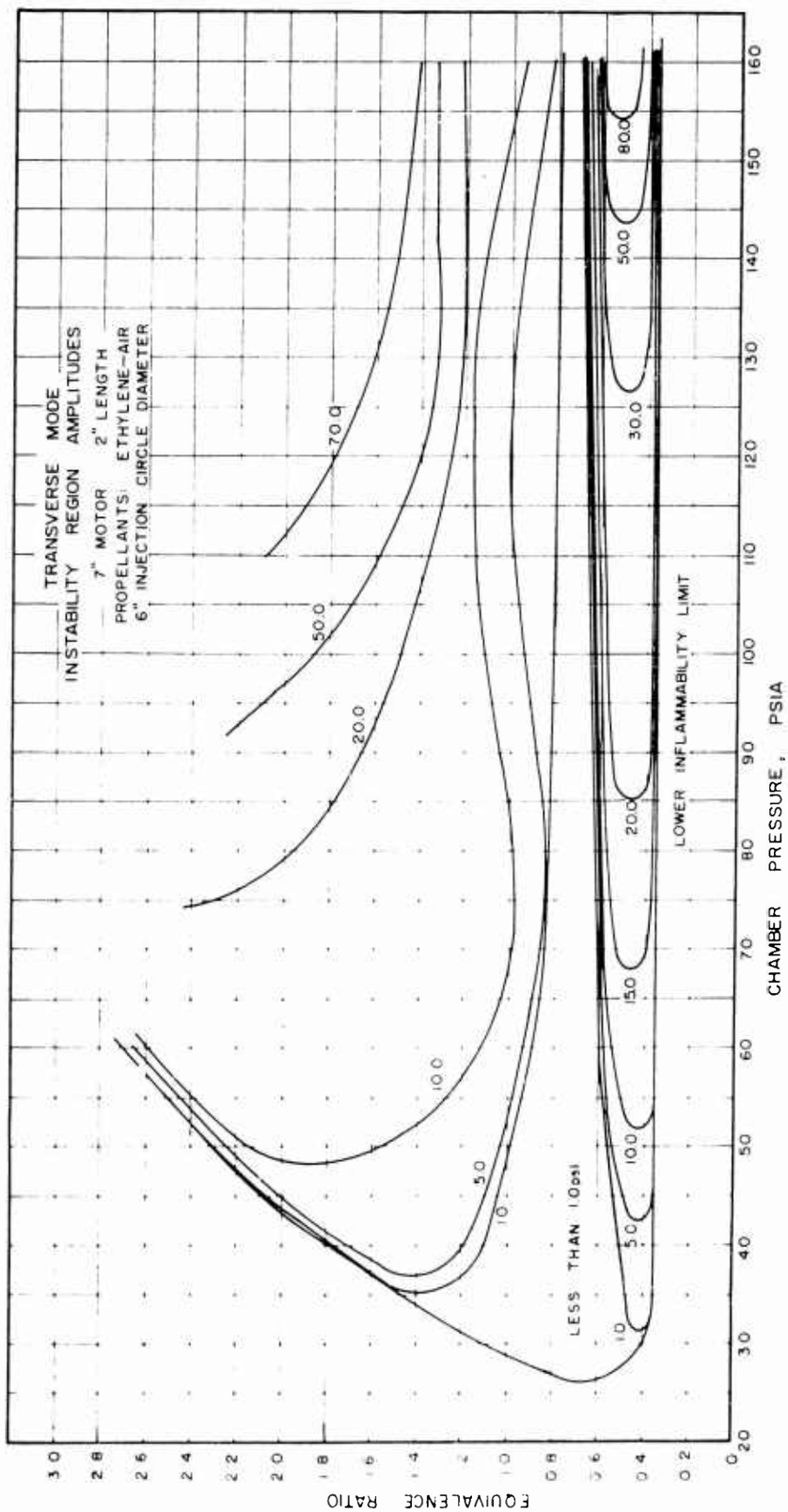

Fig. 4 Instability Region and Amplitudes

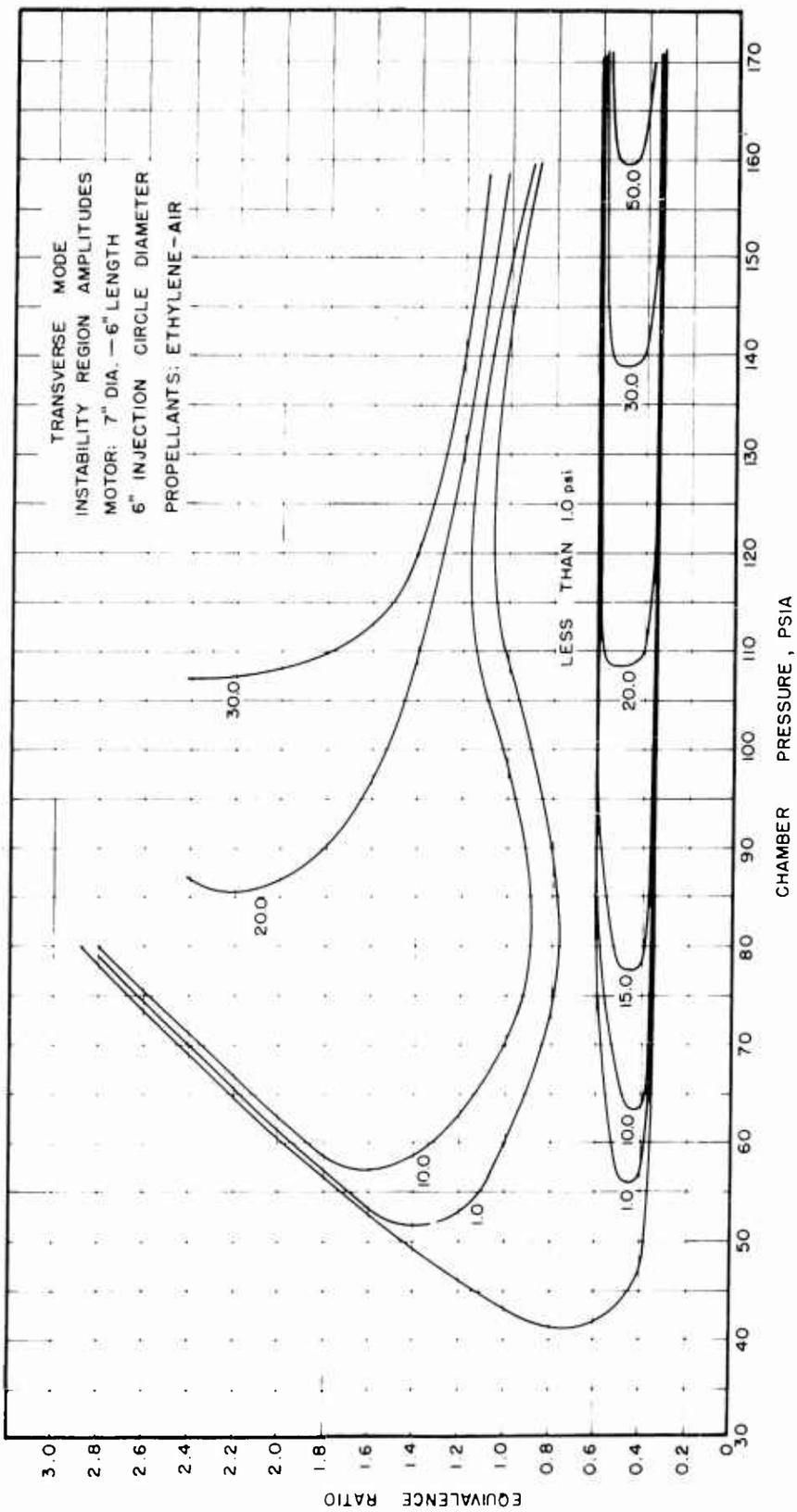

Fig. 5 Instability Region and Amplitudes

chamber with the exception that no oscillations occurred until a mean chamber pressure of 42 psia was reached.*

Injector B with the injection holes on a 4 in. diameter circle was operated over the complete operating range and no combustion pressure oscillations were observed in either the 2 or 6 in. long chambers; however, rough burning** was observed in both motors when the equivalence ratio was about 1.0. Figures 6 and 7 illustrate these regions for the 2 and 6 in. motors respectively. Figure 8 is a typical oscillograph record taken during rough burning.

Figures 9 and 10 are the instability regions for injector C (2 in. diameter injection circle) for chamber lengths of 2 and 6 in. respectively. For the 2 in. length, a region of oscillations of the second radial mode (10,000 to 17,000 cps) was observed centered about an equivalence ratio slightly above 1.0. A region where oscillations of the first and second tangential modes (2000 to 5000 cps) occurred bounded the former region on the high equivalence ratio side. For the 6 in. length (see Fig. 10), the region of instability had no complex inner regions. The "toe" occurred at a chamber pressure of about 47 psia and an equivalence ratio around 1.25.

Side Injection

Figure 11 is the instability region for side injection in a 2 in. long combustion chamber. The region of instability was divided into an

---

* A complete discussion of the instability regions found using this injector with combustion chamber lengths from 2 through 12 in. is given in References (3) and (4).

** Rough burning is that type of burning where low amplitude pressure oscillations occur exhibiting no definite frequency or phase relationship.

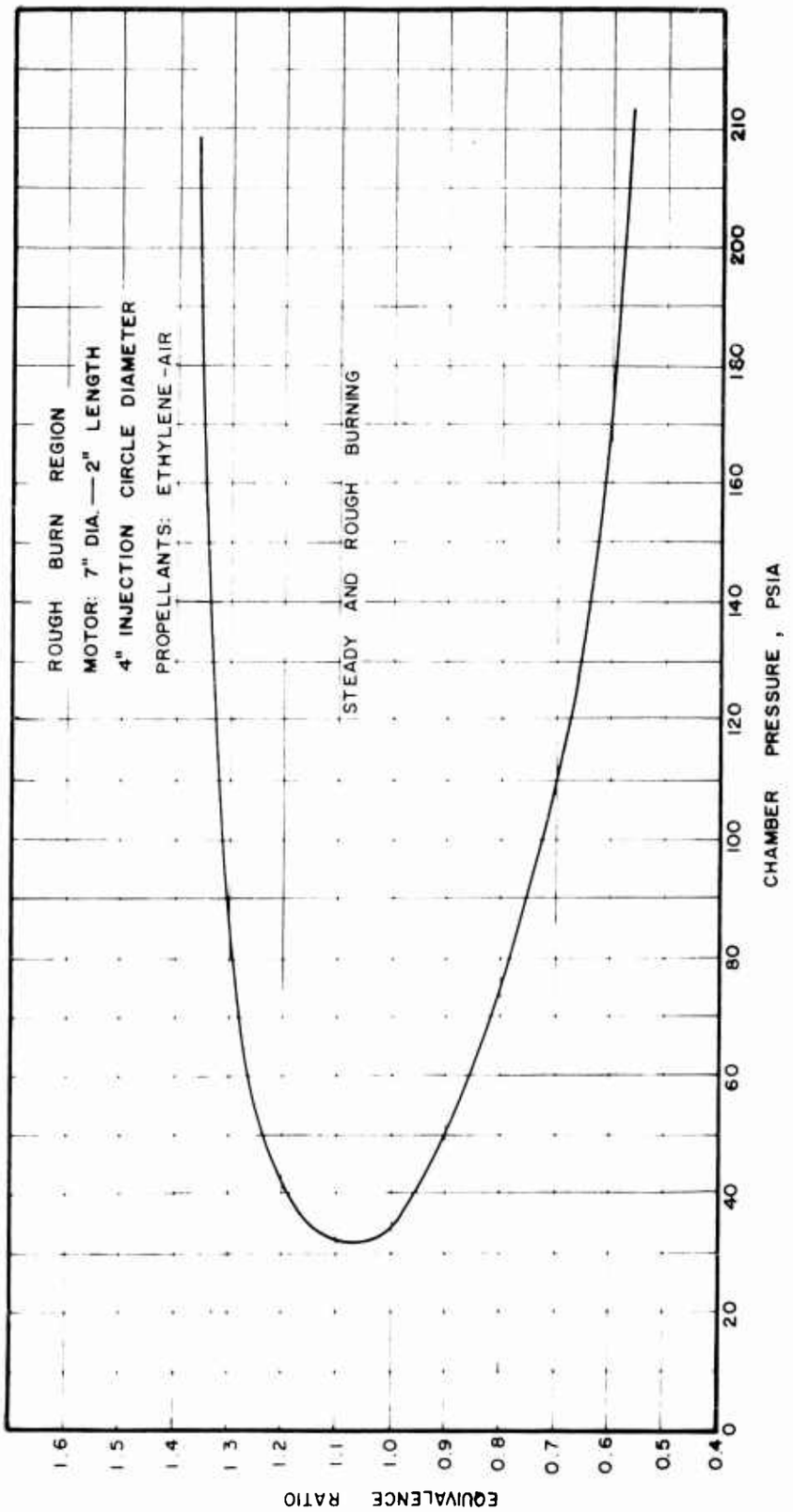

Fig. 6 Rough Burning Region

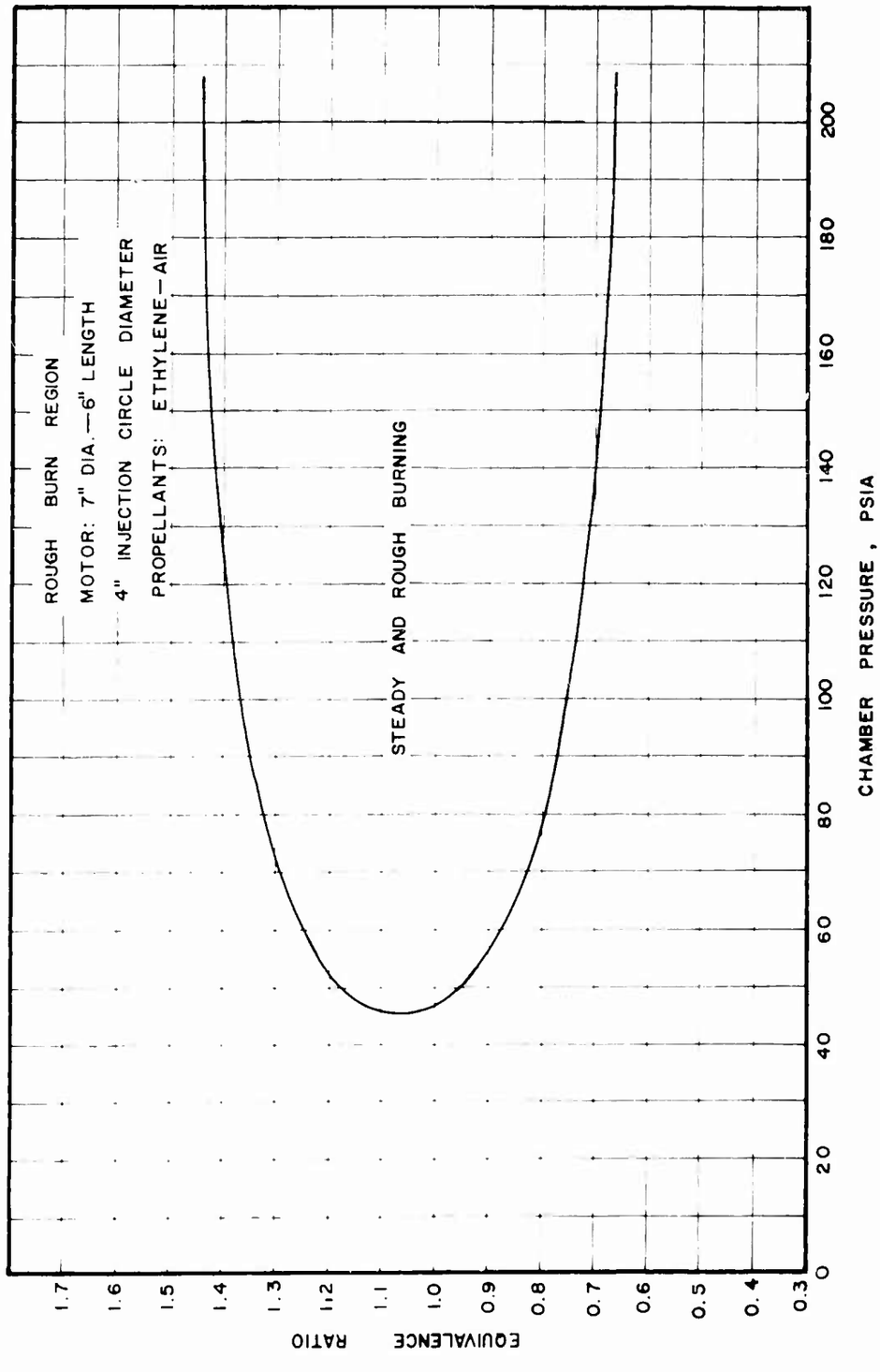

Fig. 7 Rough Burning Region

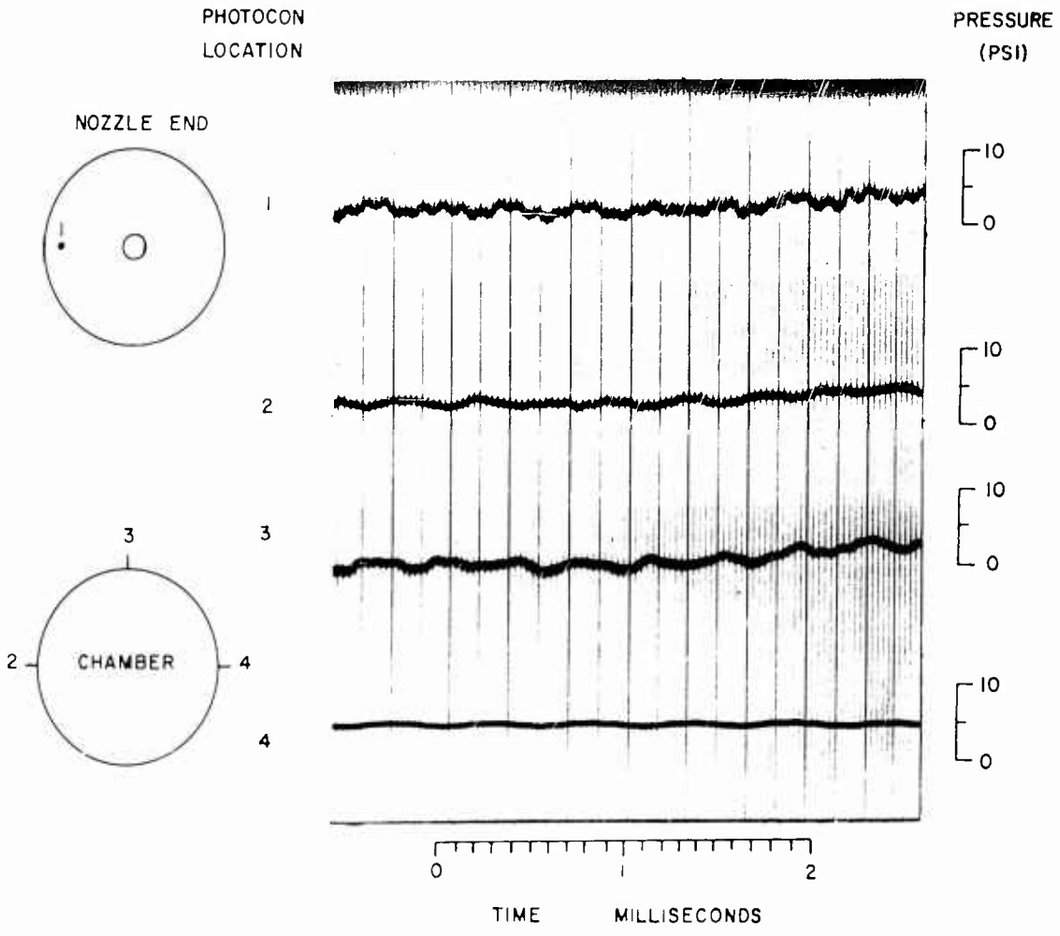

Fig. 8 Oscillograph Record of Rough Burning

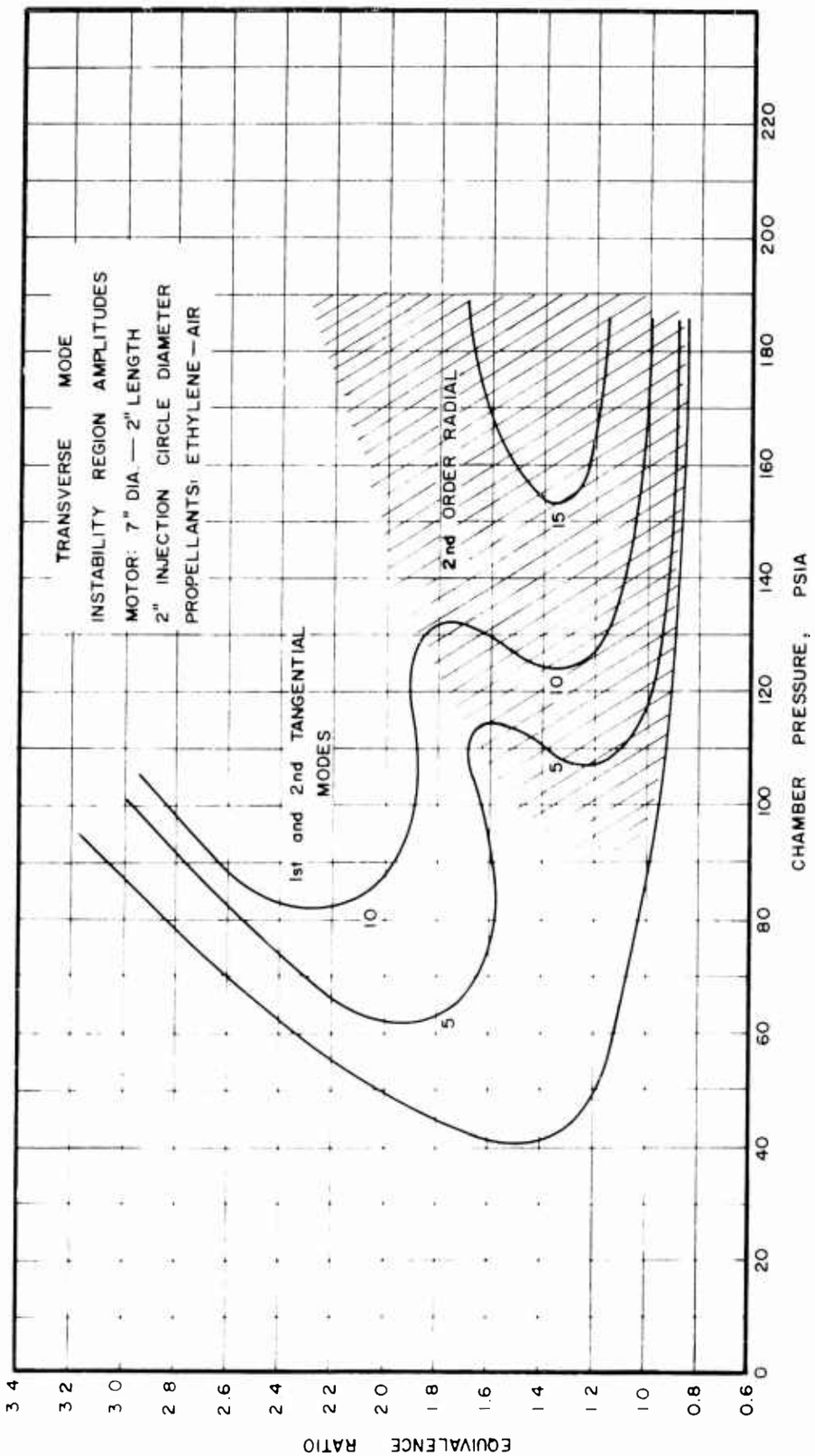

Fig. 9 Instability Region and Amplitudes

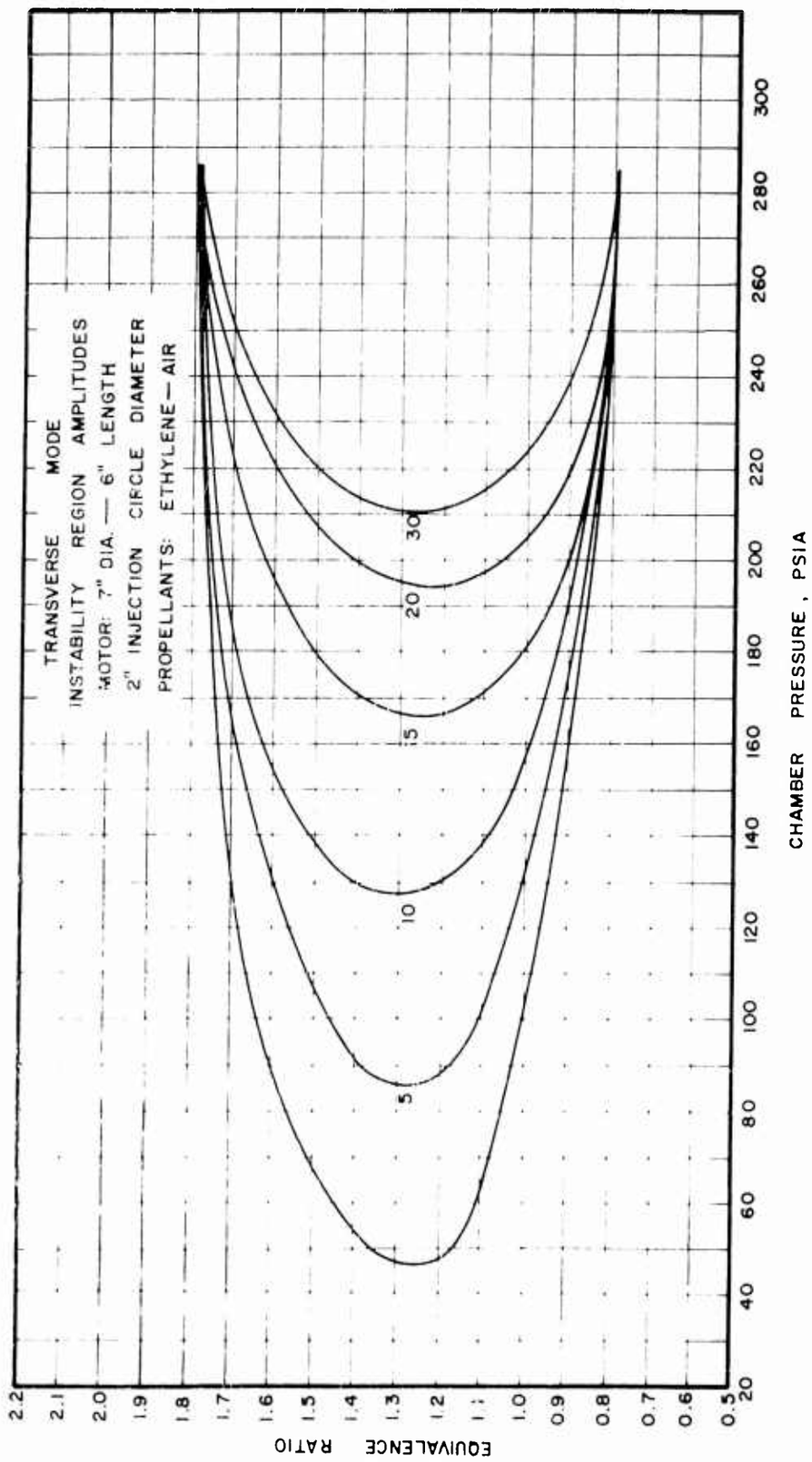

Fig. 10 Instability Region and Amplitudes

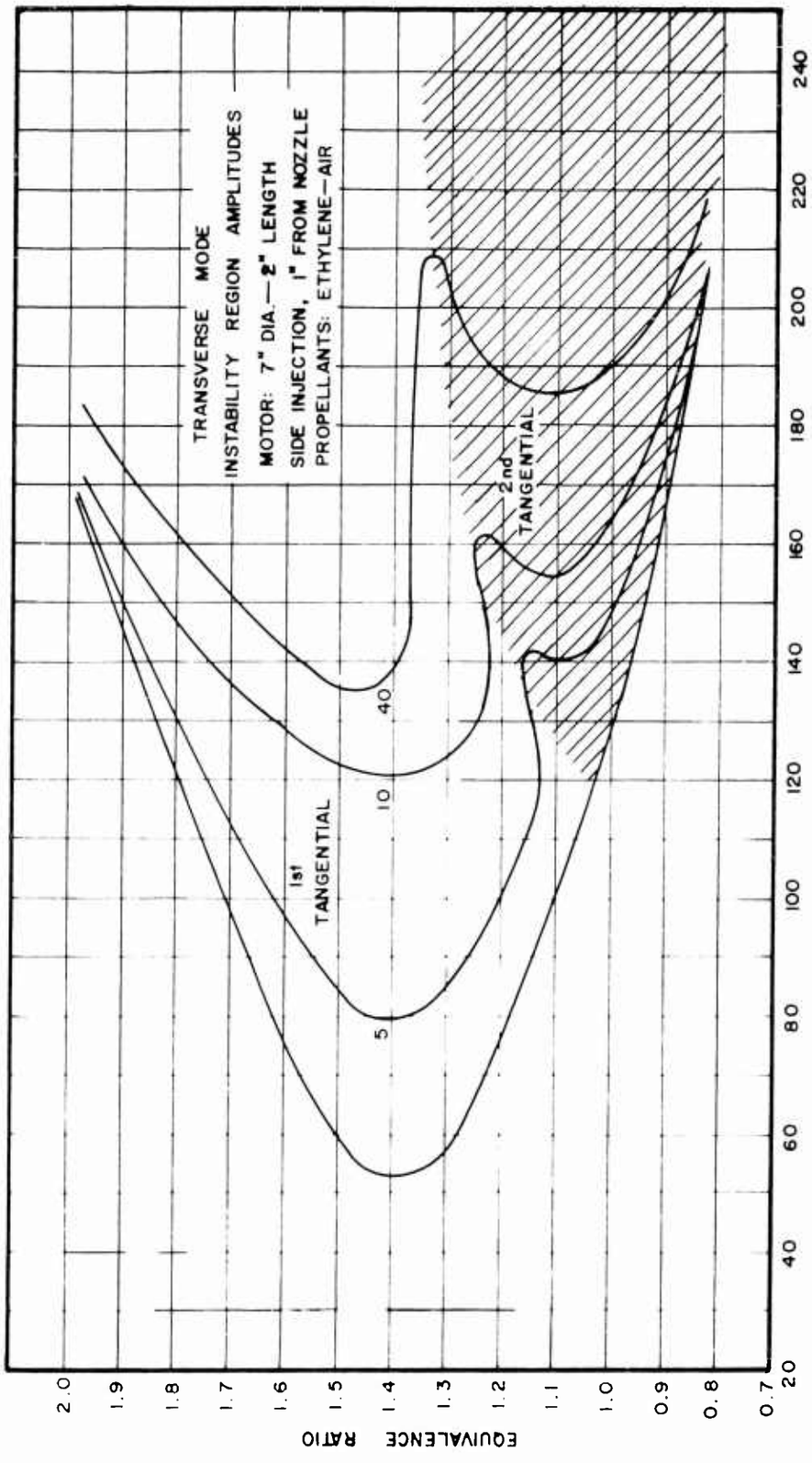

Fig. 11 Instability Region and Amplitudes

area wherein second tangential oscillations occurred and an area wherein first tangential oscillations occurred. The toe of the region occurred at an equivalence ratio of 1.4 and a mean chamber pressure of 52 psia.

No periodic combustion pressure oscillations were observed at any point of operation for the 6 in. long combustion chamber with side injection.

Figure 12 is the instability region for a 14 in. long motor with injection at a location in the side of the chamber 13 in. from the nozzle. Oscillations were observed at a mean chamber pressure as low as 20 psia. Similar results were obtained in References (5) and (6) for the head end injection system in a 3 3/8 in. diameter motor. Only stable and rough burning were observed when injecting 7 in. from the nozzle in the 14 in. long motor.

Figure 13 is the instability region for the 14 in. long motor with side injection at a location 1 in. from the nozzle. The region is similar to the one found in the experiments in which the gases were injected 13 in. from the nozzle.

Nozzle End Injection

Figures 14 and 15 are the instability regions for the experiments in which the gases were injected in the nozzle end of the combustion chambers having 2 and 6 in. chamber lengths respectively. The region for the 2 in. length was similar to the region obtained from the experiments with head end injector A and a 2 in. long chamber. The peak-to-peak amplitude of the pressure oscillations was much lower for the experiments with the nozzle end injector than for those of the head end injector. It can be recalled that the injection pattern for the nozzle

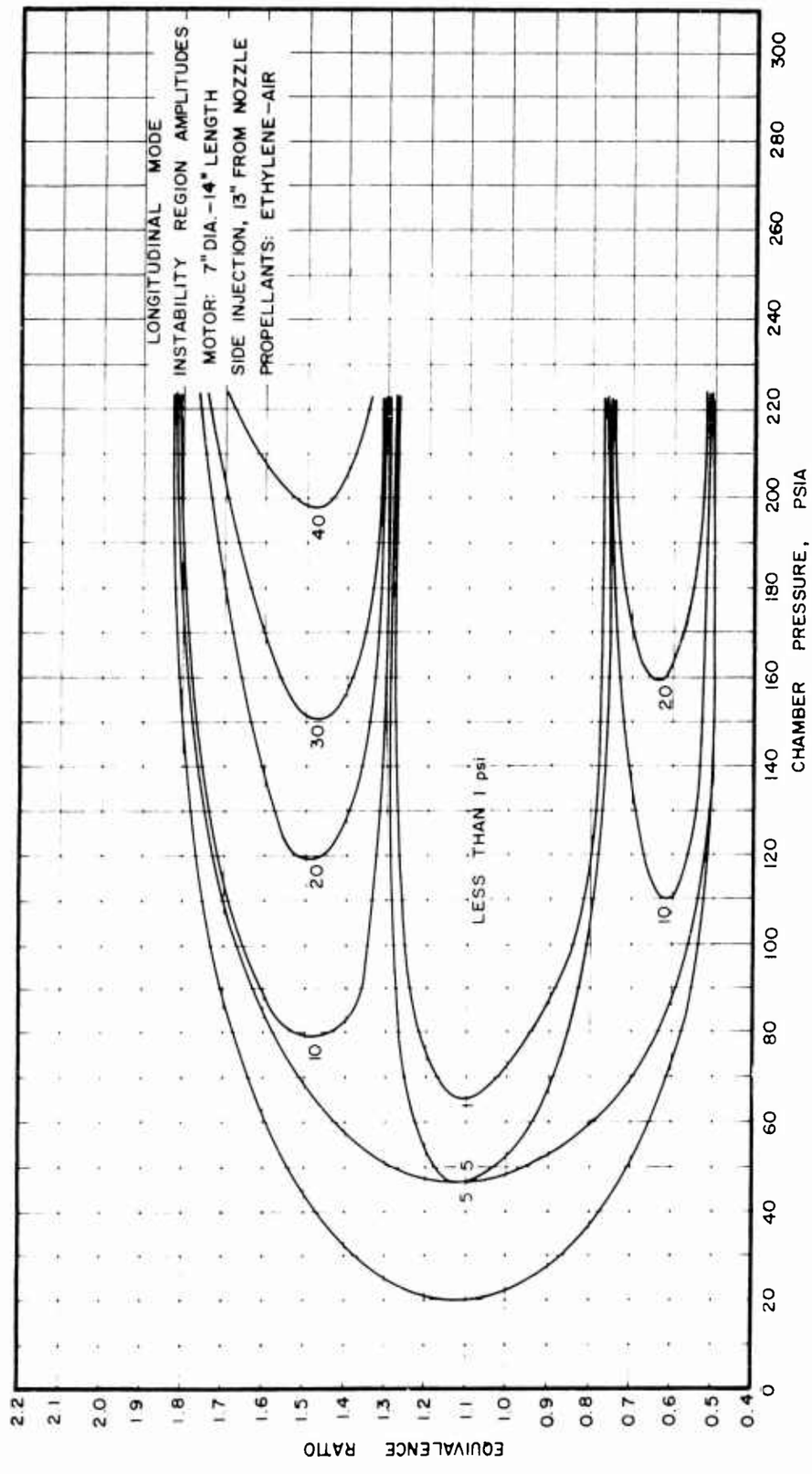

Fig. 12 Instability Region and Amplitudes

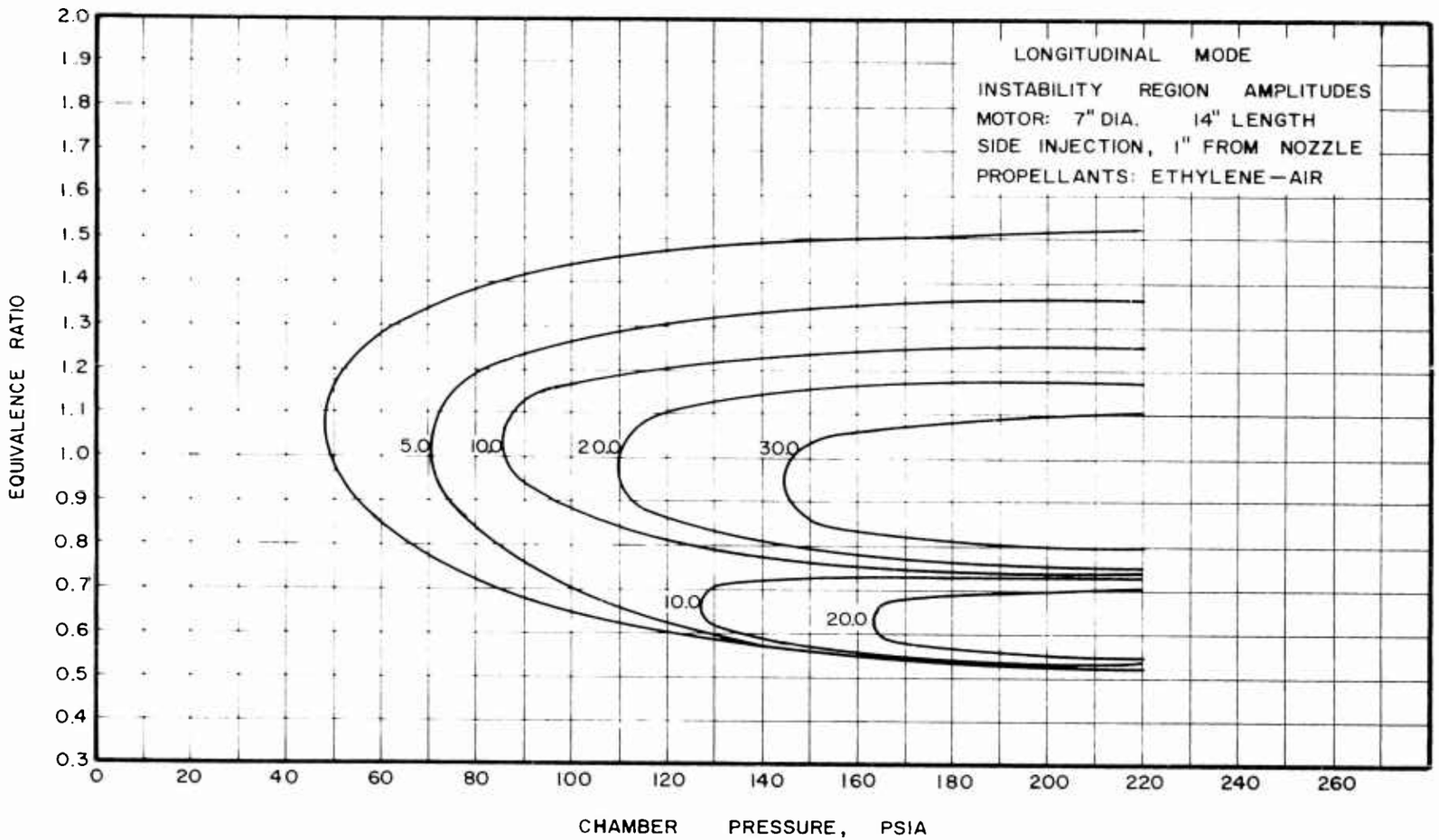

Fig. 13 Instability Region and Amplitudes

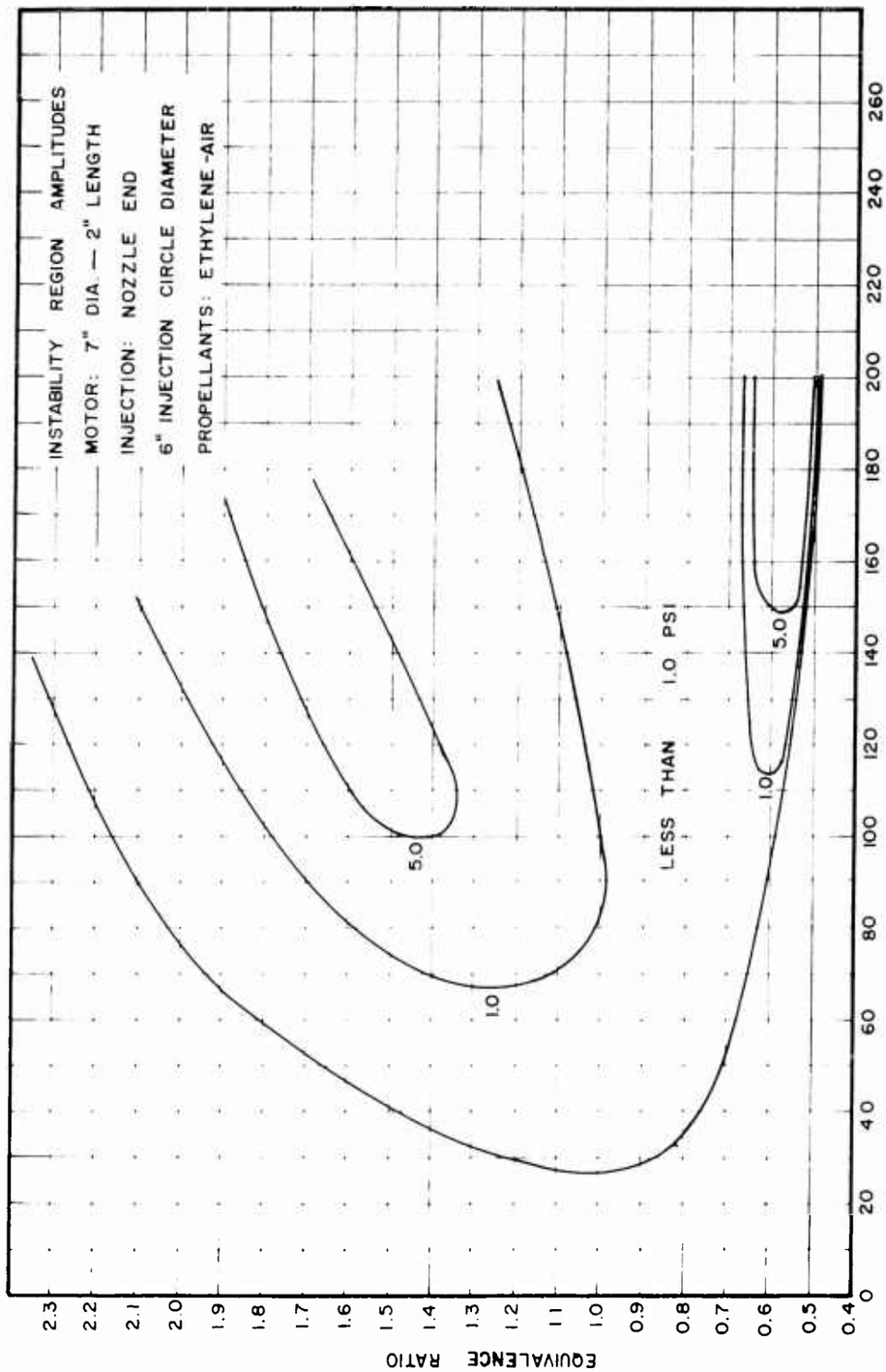

Fig. 14 Instability Region and Amplitudes

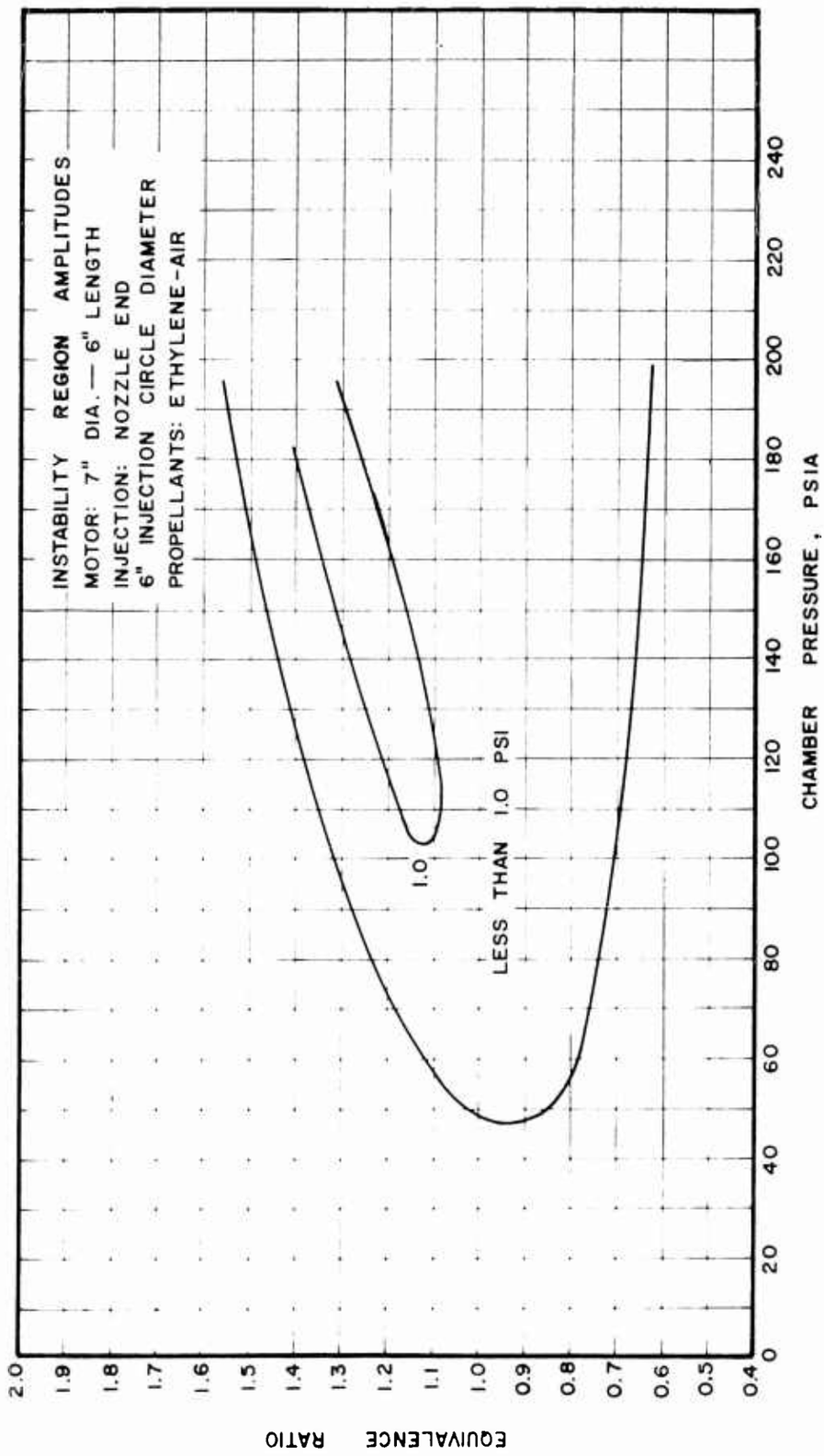

Fig. 15 Instability Region and Amplitudes

end injector was identical to that of head end injector A. The instability region for the rocket motor configuration consisting of a 6 in. long chamber and the nozzle end injection system exhibited only low (about 1.0 psid) peak-to-peak amplitude pressure oscillations.

Modes of Oscillation

Head End Injection

Only one mode of oscillation was found using injector A with both the 2 and 6 in. chamber lengths. Figure 16 is an oscillograph record of this mode of oscillation. It was identified as a first tangential or "spinning" mode by analyzing the phase relationship and frequency of the different pressure traces (see Appendix B for a discussion of the theoretical modes of oscillation). The frequency of the oscillation was 2400 cps.

As was stated in the previous section, no definite mode of oscillation was observed using injector B with either the 2 or 6 in. long combustion chambers.

Figure 17 is an oscillograph record of the high frequency oscillations which occurred in a 2 in. long combustion chamber using injector C. An analysis of Fig. 17 indicates that the frequency of oscillation is 11,800 cps. The frequency and phase relationship of the different pressure traces indicate that the above mode of oscillation is a second radial mode. This type of mode occurred using injector C in a 2 in. long chamber for fuel-air ratios approximately equal to the stoichiometric value (see Fig. 9). The other modes most frequently observed for this motor were the first and second tangential modes (see Figs. 9, 16, and 19).

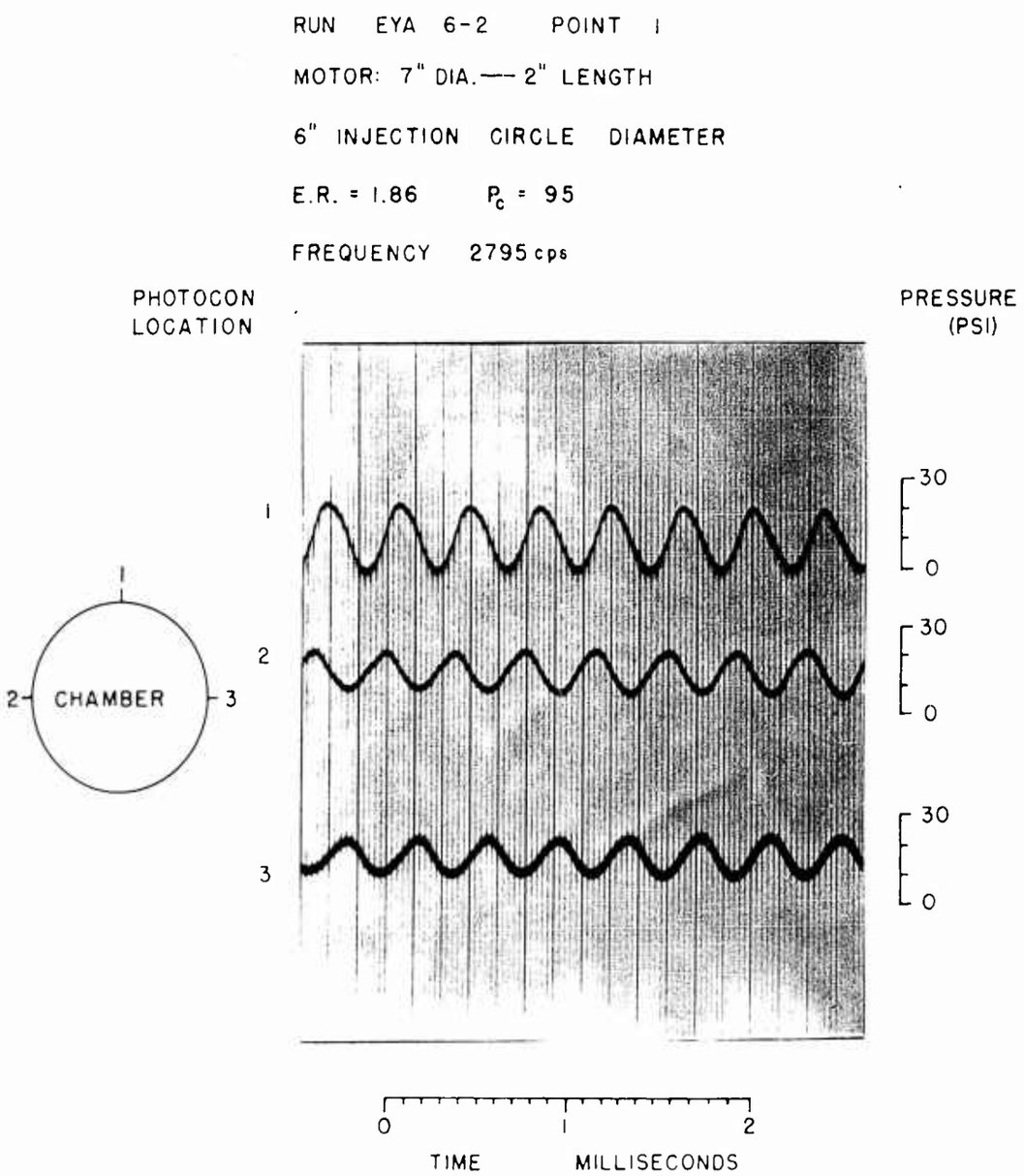

Fig. 16 Oscillograph Record of the First Tangential Mode

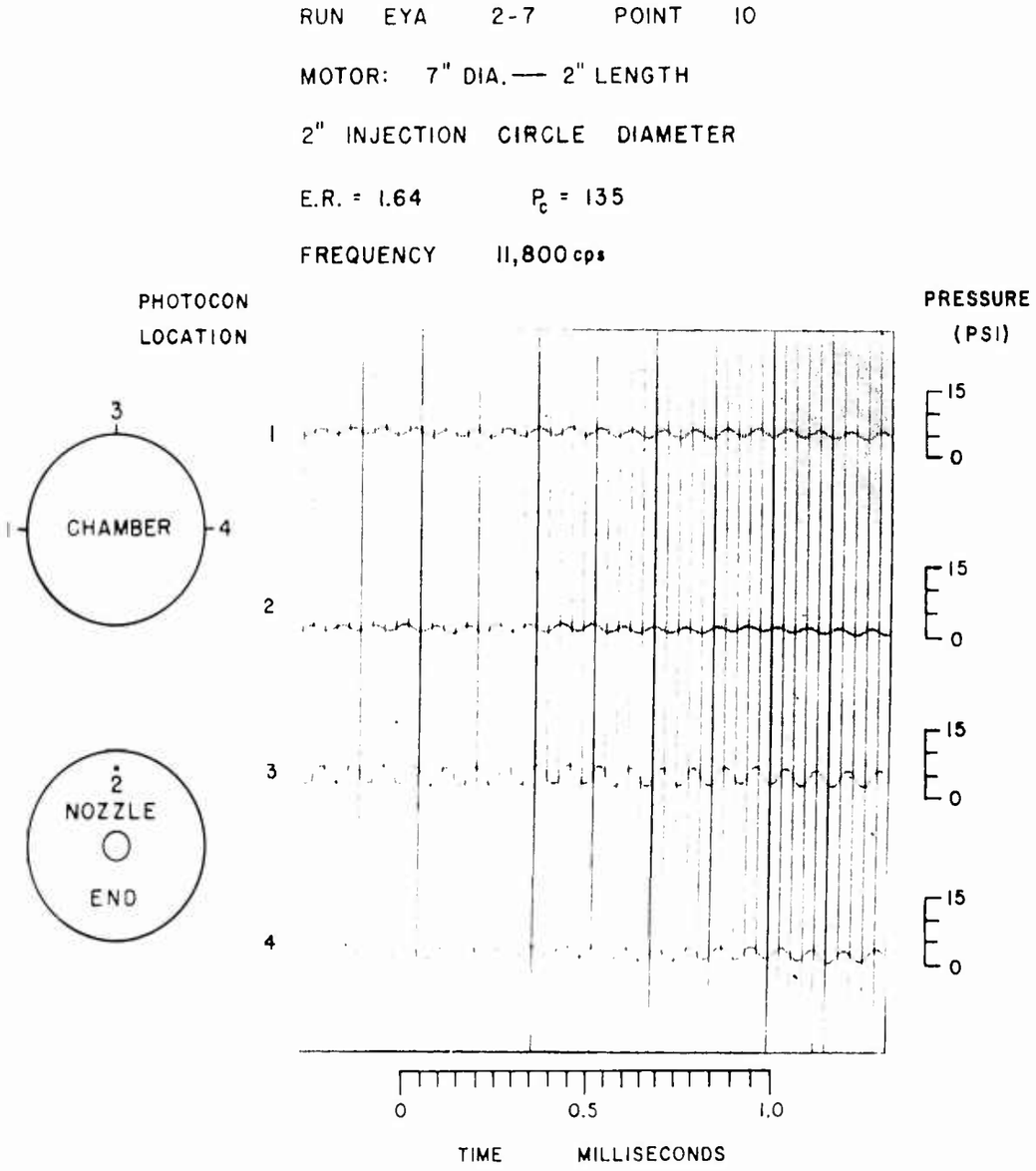

Fig. 17 Oscillograph Record of the Second Radial Mode

A first radial mode was the only mode of oscillation observed for the experiments using injector C with a 6 in. long chamber. Figure 18 is an oscillograph record of this oscillation. An analysis of the record indicates that all four pressure traces are in phase and that the frequency of oscillation is 5200 cps. This corresponds to the radial mode.

Side Injection

The first and second tangential modes were the two modes observed when injecting in the side of a 2 in. long chamber. A first tangential mode is shown in the oscillograph record presented by Fig. 16. An oscillograph record of a second tangential mode is shown on Fig. 19. The latter oscillograph record indicates that the pressure oscillation at location 1 (see the left side of Fig. 19) is in phase with the oscillation at location 3 and out of phase with that at location 2. This indicates that two waves are "spinning" in the chamber (see Fig. 25). Trace 4 indicates no pressure oscillations in the center of the chamber.

Figure 20 is an oscillograph record of a first tangential mode with a radial mode superimposed on the tangential mode. In this case the transducer located in the center of the chamber (number 4) sensed only the radial mode, while the other three sensed both modes.

As was stated in the previous section, no pressure oscillations were observed when injecting at any of the three injection locations in the side of a 6 in. long motor.

Longitudinal and radial oscillations were observed for the experiments with the 14 in. long chamber having side injection 13 in. from the nozzle. Figure 21 is an oscillograph record of a longitudinal mode

RUN EYA 2-15-6 POINT 29
MOTOR: 7" DIA. — 6" LENGTH
2" INJECTION CIRCLE DIAMETER
FREQUENCY 5200 cps
E.R. = 1.51 P_c = 175 psia

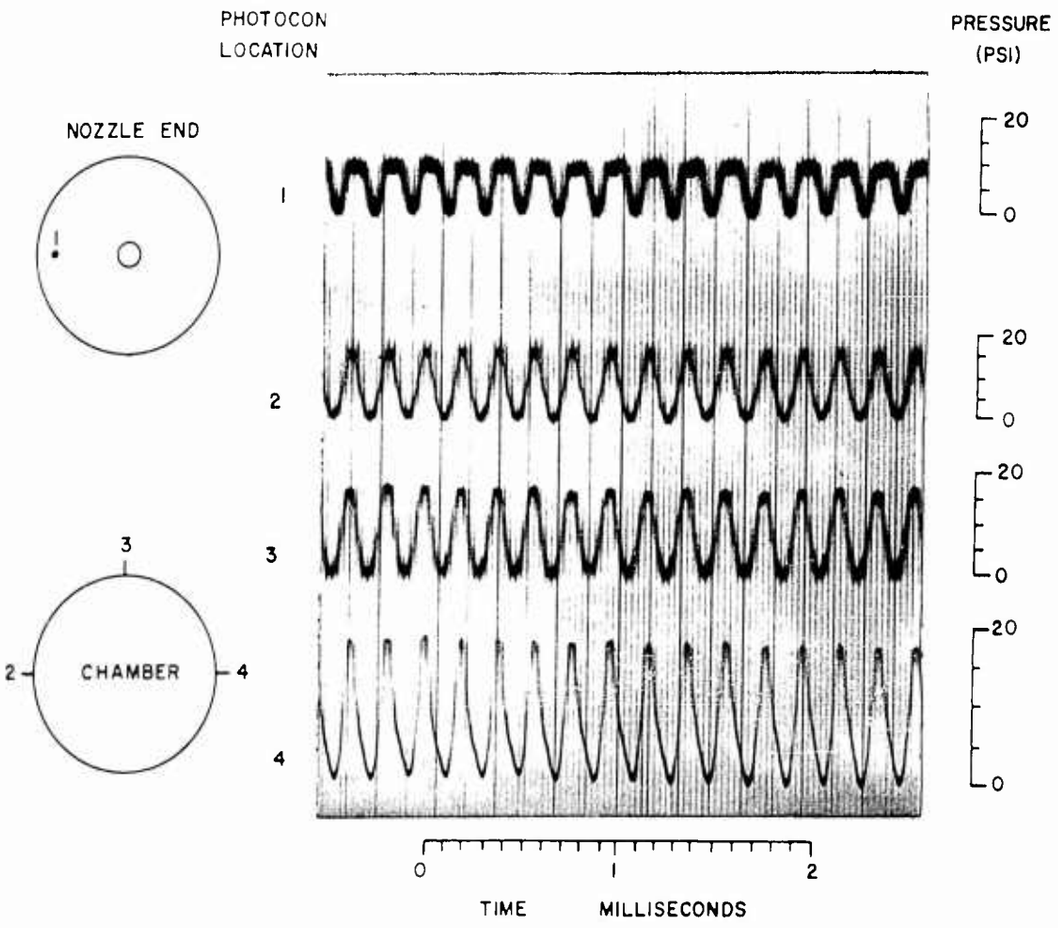

Fig. 18 Oscillograph Record of the First Radial Mode

RUN EYA-2S-2-1 POINT 17
MOTOR: 7" DIA. - 2" LENGTH
SIDE INJECTION, 1" FROM NOZZLE
FREQUENCY 4500 cps
E.R. = 1.20 P_c = 147 psia

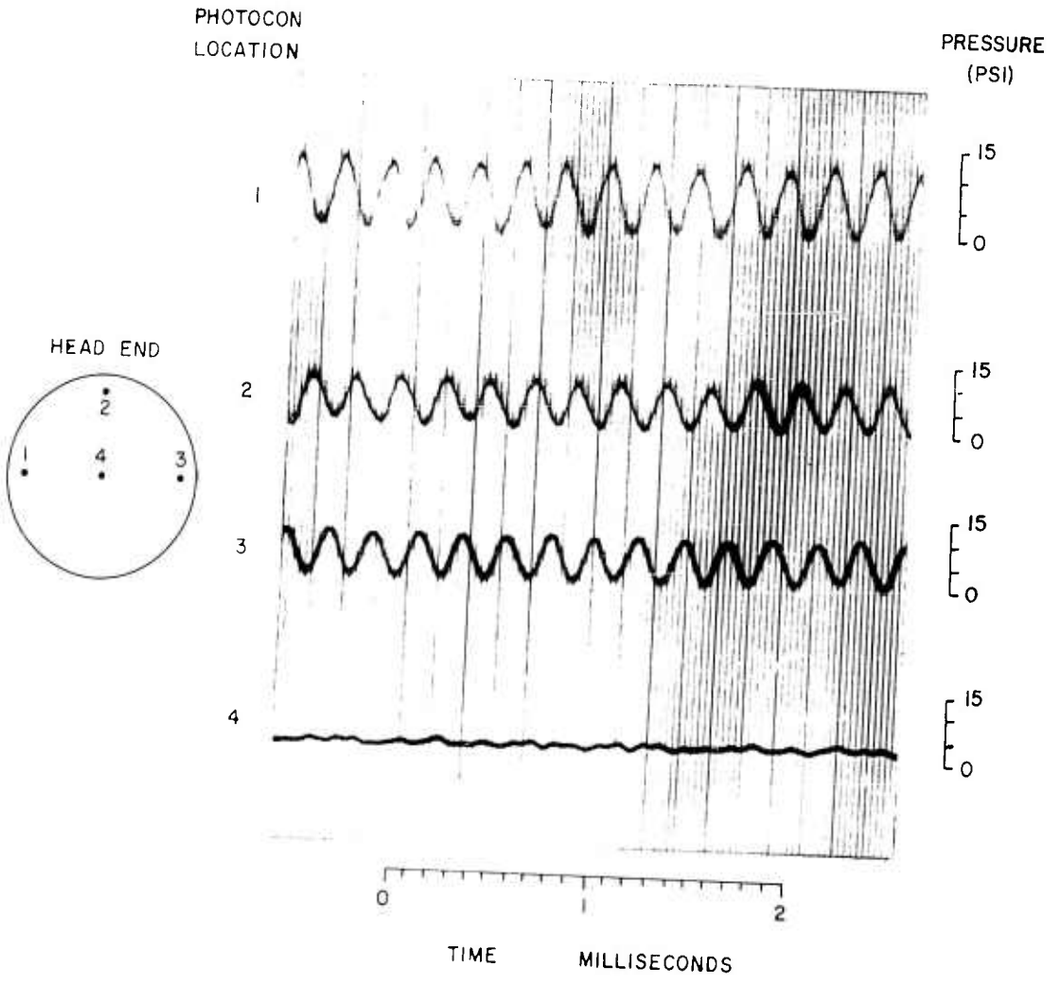

Fig. 19 Oscillograph Record of the Second Tangential Mode

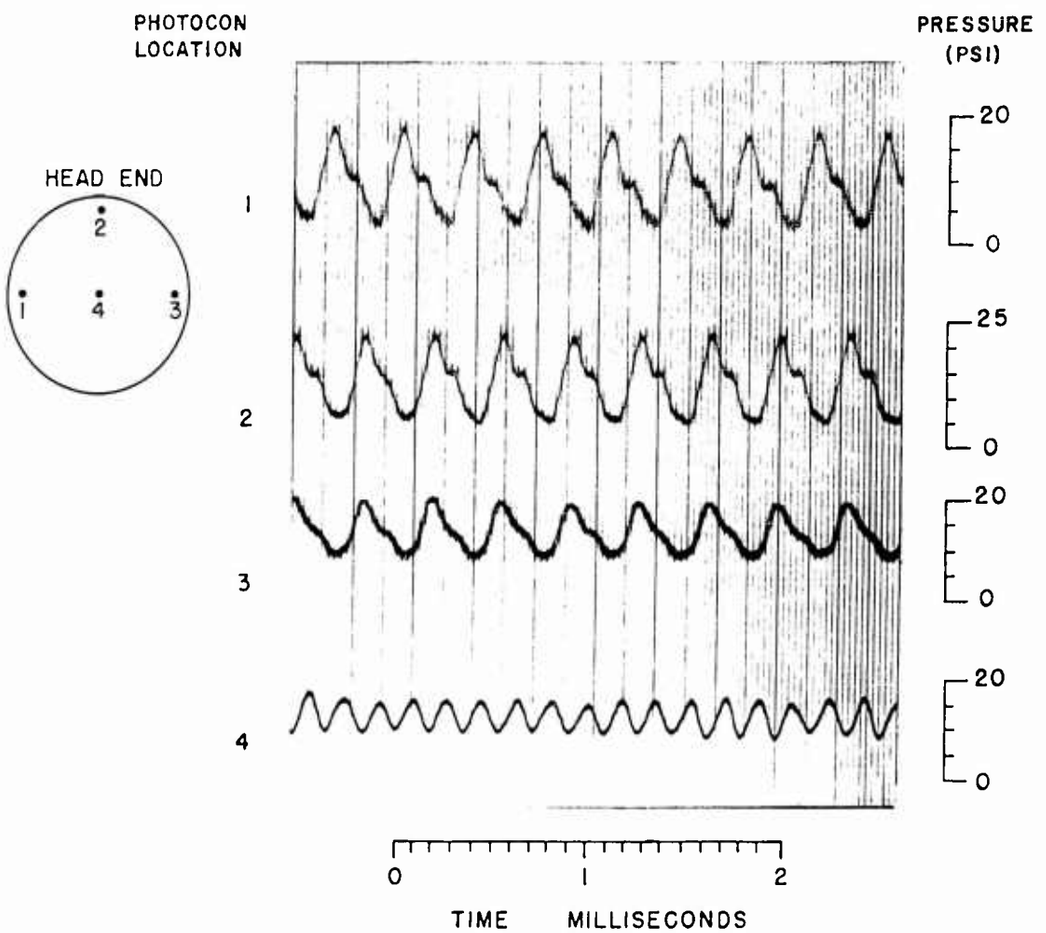

Fig. 20 Typical Oscillograph Record of the Superimposed Modes

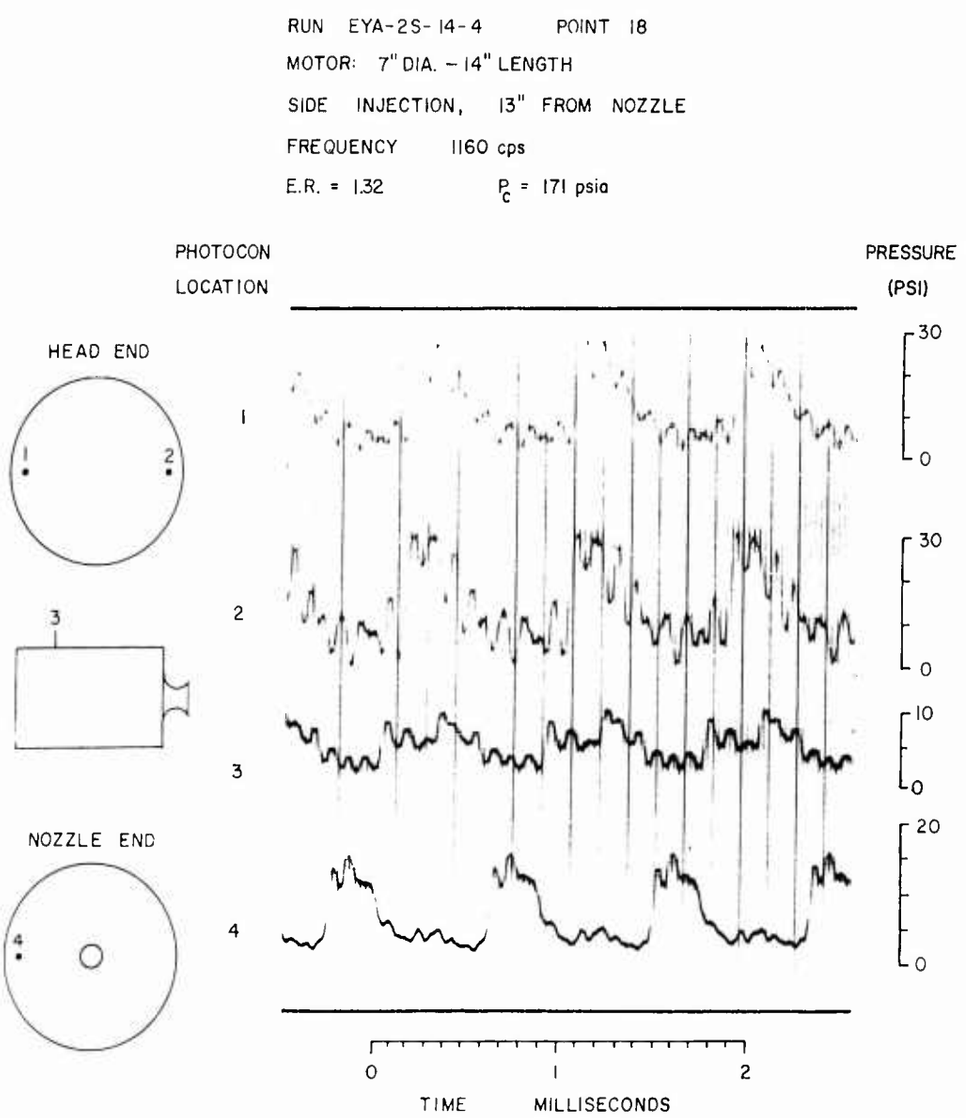

Fig. 21 Oscillograph Record of the Longitudinal Mode

with a superimposed radial mode. An investigation of the oscillograph record indicates that the longitudinal mode had a frequency of 1160 cps and the radial mode had a frequency of about 10,000 cps.

Longitudinal and radial oscillations were also observed in the 14 in. long motor with injection in the side of the chamber 1 in. from the nozzle, while no oscillations were observed when injecting 7 in. from the nozzle.

Nozzle End Injection

The mode of oscillation observed when injecting in the nozzle end of the motor was the first tangential mode. This mode was observed in both the 2 and 6 in. long chambers. It is of interest to note that this mode was also observed when injecting in the head end with injector A (see Fig. 16).

Summary of Results

Table 1 on the following page presents a summary of the results found in this investigation indicating which injection scheme supported which mode of oscillation.

Peak-to-Peak Amplitudes of the Pressure Oscillations

Figures 22, 23, and 24 are graphs of the peak-to-peak amplitudes of the pressure oscillations observed. These were the maximum amplitudes observed at a given chamber pressure for any value of equivalence ratio or mode of oscillation. Figure 22 is for the 2 in. long chamber, Fig. 23 for the 6 in. and Fig. 24 for the 14 in. chamber.

From Fig. 22 (2 in. long chamber) it can be seen that injection from the head end near the periphery of the chamber caused higher amplitude

Table 1 Table of Results

MOTOR	MODE
1 HEAD END INJECTION	
(a) 6" CIRCLE, 2" LENGTH	1st TANGENTIAL
(b) 6" CIRCLE, 6" LENGTH	1st TANGENTIAL
(c) 4" CIRCLE, 2" & 6" LENGTH	STABLE & ROUGH BURNING
(d) 2" CIRCLE, 2" LENGTH	1st & HIGHER ORDER RADIAL & TANGENTIAL
(e) 2" CIRCLE, 6" LENGTH	RADIAL
2 SIDE INJECTION	
(a) 2" LENGTH, 1" FROM NOZZLE	1st & 2nd TANGENTIAL
(b) 6" LENGTH, 5" FROM NOZZLE	STABLE BURNING
(c) 6" LENGTH, 3" FROM NOZZLE	STABLE BURNING
(d) 6" LENGTH, 1" FROM NOZZLE	STABLE BURNING
(e) 14" LENGTH, 13" FROM NOZZLE	1st LONGITUDINAL
(f) 14" LENGTH, 7" FROM NOZZLE	STABLE & ROUGH BURNING
(g) 14" LENGTH, 1" FROM NOZZLE	1st LONGITUDINAL
3 NOZZLE END INJECTION	
(a) 6" CIRCLE, 2" LENGTH	1st TANGENTIAL
(b) 6" CIRCLE, 6" LENGTH	1st TANGENTIAL

Fig. 22 Pressure Oscillation Amplitude vs. Chamber Pressure

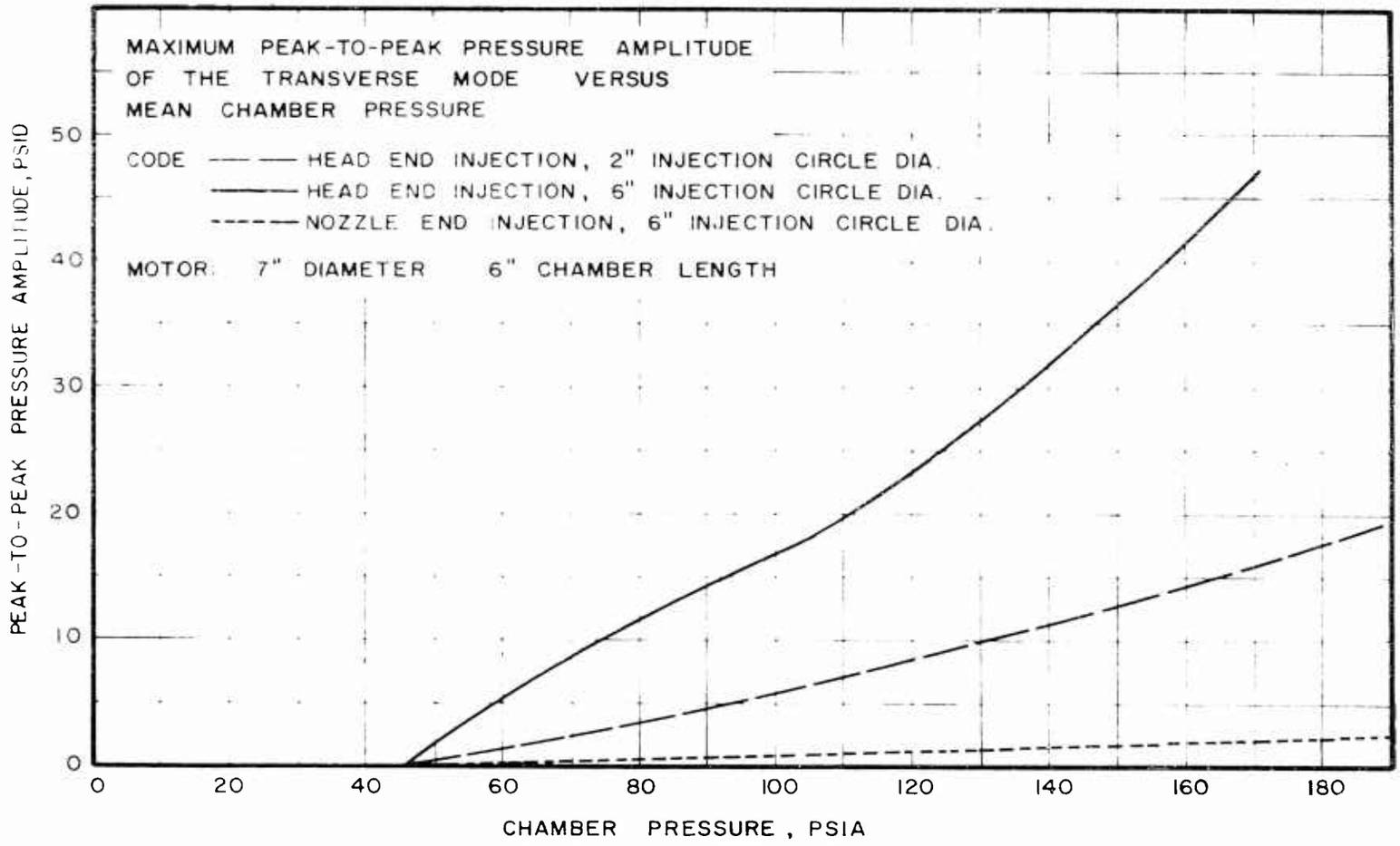

Fig. 23 Pressure Oscillation Amplitude vs. Chamber Pressure

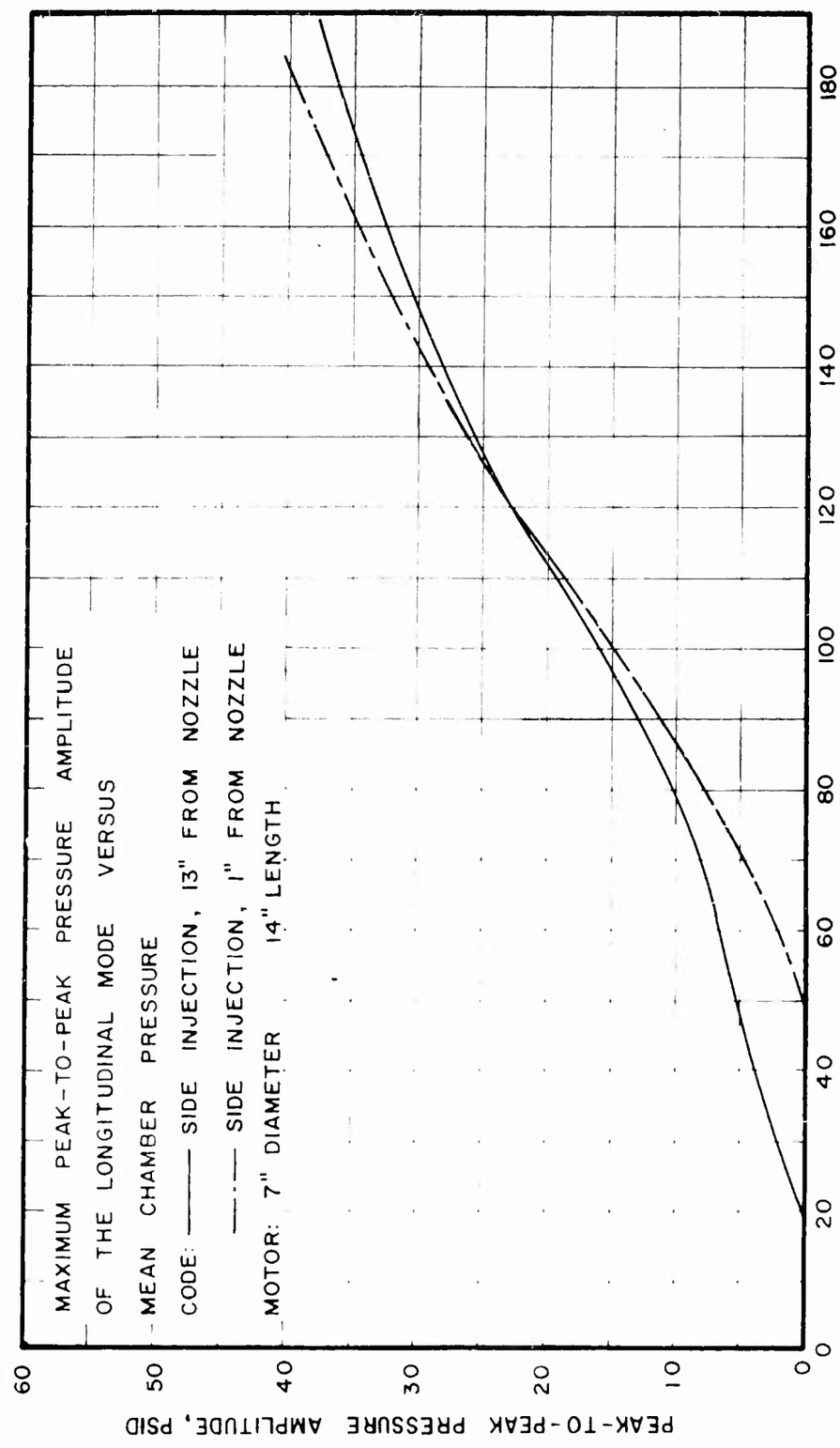

Fig. 24 Pressure Oscillation Amplitude vs. Chamber Pressure

oscillations for a given mean chamber pressure than the other injection schemes. That is, injection from the nozzle end of the chamber with an identical injection pattern caused much lower amplitude oscillations, as did injection from the side. Similar results are shown in Figs. 23 and 24.

DISCUSSION OF RESULTS

The Nature of Combustion Pressure Oscillations

A brief description of the driving mechanism of combustion pressure oscillations will help in the discussion of the results obtained in this investigation. It is generally agreed that the mechanism by which both longitudinal and transverse combustion pressure oscillations are driven can be explained in the following manner. A small pressure wave initiated by some disturbance such as the reaction zone itself passes through the reaction zone and locally increases the pressure and temperature of the burning and unburned propellants. The increase in temperature and pressure causes an increase in the chemical reaction immediately behind the pressure wave. This increase in chemical reaction tends to drive and amplify the pressure wave. The pressure wave would continue to grow if sufficient energy were released in the gases through which it was passing. In most cases, however, the amount of energy available to drive and amplify the pressure wave is limited due to the type of propellants burned and the rate at which they are supplied. If the pressure wave makes a complete cycle before sufficient fresh propellants are injected into the chamber, the pressure wave cannot receive more energy and the wave will die out. On the other hand, if the propellants are injected rapidly, the pressure wave may receive enough energy to be amplified, and it may even be possible for more than one modal type of wave to be supported.

Head End Injection

Head End Injection Near the Periphery of the Chamber

The results of the head end injection studies indicated that injection near the periphery of the chamber using injector A supported a "spinning" mode (see Fig. 25) in both the 2 and 6 in. long chambers. This mode was amplified since the energy was supplied where the pressure waves of the "spinning" mode could obtain the additional energy needed. That is, the energy was supplied at the location where the pressure variation was a maximum. Injection near the periphery should also support a radial mode since the radial pressure oscillation was a maximum in the zone of chemical reaction. The frequency of the radial mode, however, was higher than the frequency of the "spinning" mode. As a result, the radial mode required more energy because the wave travel time was shorter. That is, its pressure wave returned to the combustion zone more frequently than did that of the "spinning" mode. For this reason the "spinning" mode was the mode that occurred in the tests with this injector. In some cases the heat release rate was high enough to support two waves, and a radial mode occurred which was of smaller amplitude and superimposed on the spinning" mode.

A region of high amplitude pressure oscillations occurred near the lower inflammability limit for injector A and also for the case of injection at the nozzle end (see Figs. 4, 5, and 14). An explanation of this is that at the lower inflammability limit a slight increase in the chamber pressure initiates combustion whereas a decrease in pressure may cause combustion to cease. Therefore, it is possible for a pressure

wave to travel in the chamber at the lower inflammability limit causing only localized combustion and using the available energy in the propellants solely for the propagation of the wave. This causes pressure oscillations to occur near the lower inflammability limit. If the equivalence ratio were raised slightly, combustion would occur throughout the chamber and insufficient energy would be available to support a pressure wave.

The instability region for injector A with a 6 in. chamber occurred at a higher chamber pressure than the instability region for the 2 in. length (see Figs. 4 and 5). The reason for this shift is explained in References (3) and (4) which state that as the volume of the chamber increases, the amount of energy released must increase to maintain that certain energy release rate per unit volume required for sustaining combustion pressure oscillations. This is accomplished by increasing the propellant flow rate which in turn increases the mean chamber pressure. Therefore, the instability region for a longer combustion chamber occurs in an area of higher mean combustion pressure than does one for a shorter length.

Head End Injection Near the Axial Center Line of the Chamber

With injector C, injection was near the axial center line of the chamber. The fundamental mode of oscillation using this injector was a radial mode (see Figs. 17 and 18). This was because the energy was supplied in the center of the chamber where the pressure variation for the radial mode was a maximum, while that for the "spinning" mode was a minimum. A first radial mode occurred in the 6 in. long chamber, and a second radial mode occurred in the 2 in. long chamber. The reason for

the different modes was that the heat release rate per unit volume in the 2 in. length was the larger of the two as was discussed above and in (3) and (4).

Head End Injection Between the Periphery and Axial Center Line of the Chamber

Injector B injected the premixed gases on a 4 in. diameter injection circle. Both the 2 and 6 in. long motors were stable when using that injector. Occasional transient radial and tangential modes were observed in the 2 in. chamber where the heat release rates were high (3) (4), but none of the oscillations was self sustaining. A possible explanation of this is that symmetrical injection, midway between the center and periphery, supplies the energy to the chamber in such a location that it favors neither mode of oscillation. That is, the oscillations compete equally with one another for the available energy in the combustion zone, and neither receives enough to sustain itself. It is conceivable, then, that both the radial and tangential modes could be supported at mean chamber pressures above 200 psia where the energy available per unit volume is higher than was obtainable in this investigation.

Side Injection

General Discussion

Injection in the side of the chamber made it possible to study the effects of injection direction and of injection location at different distances from the nozzle on the combustion pressure oscillations.

Side Injection With a 2 in. Long Combustion Chamber

Injection in the side of a 2 in. long motor caused the same "spinning" mode of oscillation that occurred with the head end injector that had a 6 in. diameter injection circle. This was because both injectors provided energy near the periphery of the chamber where the pressure variation for the "spinning" mode was a maximum. One difference in the instability regions for these two injectors was that the instability region for the side injection system had an area near a stoichiometric fuel air ratio where the second tangential mode occurred. This type of oscillation was made possible by the velocity distribution of the injection system partially reinforcing that of the acoustic mode (see Fig. 25). Another difference was that the side injection motor did not have a region of high amplitude oscillations near the lower inflammability limit (see Figs. 4 and 11).

Side Injection With a 6 in. Long Combustion Chamber

Changing the length of the combustion chamber had a profound effect on the combustion pressure oscillations. Side injection in a 6 in. long chamber caused no instability, but previously in a 2 in. long chamber high amplitude transverse combustion pressure oscillations occurred. The reason for this difference was that the heat release rate per unit volume was lower in the 6 in. long chamber than in the 2 in. long chamber. Moreover, with the side injection system, the propellants were injected toward the axial center of the chamber and tended to oppose the velocity distribution for the tangential mode (see Fig. 25). Thus, the dissipative effects of side injection were larger than for a comparable system with head end injection for that mode. Head end injection near

the periphery, however, caused a cylindrical chemical reaction zone near the outer wall where the transverse pressure oscillations were a maximum and a velocity distribution which did not directly oppose the velocity distribution of a tangential mode. Thus, side injection did not support transverse modes of combustion instability as readily as head end injection near the periphery of the chamber.

It can be concluded that the combination of the chemical reaction zone, the velocity distribution for the oscillations, and the larger volume of the 6 in. long chamber created a situation where no transverse oscillations were self-sustaining for the side injection system.

Side Injection With a 14 in. Long Combustion Chamber

Side injection near either end of the combustion chamber caused high amplitude longitudinal oscillations because the chemical reaction zone was confined by the side injection system to the ends of the chamber where the longitudinal pressure variations were a maximum. The longitudinal pressure variations are a maximum at the ends of the combustion chamber because of a reflection phenomenon at the ends of the chamber. This phenomenon is discussed in References (9) and (10) which state that the reflected pressure wave from the ends of the chamber adds to the local pressure which has not yet decayed to the mean value of the chamber. This causes a build-up of the pressure variation at the ends of the chamber. Side injection at the ends of the chamber therefore supplied energy where the pressure waves could obtain the maximum energy available.

Side injection 7 in. from the nozzle in the 14 in. long motor supplied the energy to the system where the longitudinal pressure variations

were a minimum. The energy that the pressure wave received from the burning propellants was, therefore, smaller than if injection had been at the ends of the chamber, and no combustion pressure oscillations were observed when injecting at that location. In addition to this, the distance from the chemical reaction zone to either end of the combustion chamber was less than the "lower critical length;"* therefore the pressure wave traveled from the zone of chemical reaction to the end of the chamber and reflected back again before sufficient fresh propellants could be injected into the chamber to support the pressure wave. Moreover, since it is possible that the recently injected and unburned propellants flowed both upstream and downstream into burned gases, the available energy per unit volume was too small for sustaining longitudinal pressure waves.

Nozzle End Injection

General Discussion

Injection in the nozzle end of the chamber was limited to the injection pattern in injector A of Fig. 3 because of the presence of the nozzle. That injection pattern was chosen so that a comparison could be made between nozzle end injection and head end injection.

Comparison of Nozzle End Injection to Head End Injection

The mode of combustion pressure oscillations observed for the head end injection pattern was also observed for the nozzle end injection

---

* The "lower critical length" is the length below which no longitudinal combustion pressure oscillations occur for a given rocket motor, propellant combination, and head end injection.

pattern. The amplitude of the oscillations, however, were much less with the nozzle end injector (see Figs. 22 and 23). In fact, the amplitude of the oscillations in the 6 in. long chamber was never greater than 3.0 psid. A possible explanation for this is that the combustion gases in the motor having injection in the nozzle end were forced to traverse the chamber approximately twice. Since the injector and nozzle were at the same end of the motor, the burning propellants near the injector were diluted with burned gases as they moved toward the nozzle. This caused less energy to be available for sustaining the pressure oscillations.

CONCLUSIONS AND RECOMMENDATIONS

From the results of this investigation the following conclusions were made for the 7 in. diameter rocket motor:

(1) By the choice of the proper injection location and pattern, stability or instability can be predicted.

(2) If the burning is unstable, the mode of oscillation can be predicted.

  (a) Head end injection near the periphery of the chamber tends to drive a tangential mode of oscillation.

  (b) Head end injection near the center of the chamber tends to drive a radial mode of oscillation.

  (c) Side injection near either end of a combustion chamber that is longer* than the "lower critical length" causes high amplitude longitudinal oscillations.

(3) Injection in the nozzle end of the chamber causes much lower amplitude oscillations than does head end injection.

(4) The injection schemes that do not support combustion pressure oscillations are:

  (a) Injection in the head end of the motor through holes located on a circle concentric with the outer periphery

---

* It is conceivable that an upper limit on the length of the chamber exists at which length no longitudinal oscillations will occur (see References (2), (5), and (6).

of the combustion chamber with the diameter of the circle of holes half the diameter of the combustion chamber.

(b) Injection in the side of a combustion chamber which has a length to diameter ratio of approximately 1.0.

(c) Side injection at the mid-point between the nozzle and head end of a 14 in. long combustion chamber.

For a better understanding of injection effects on combustion instability, the following investigations should be made:

(1) An investigation of injection velocity.

(2) An investigation of injection from the head end of the combustion chamber with a semi-porous injector.

(3) An investigation of the effects of propellant mixing.

BIBLIOGRAPHY

BIBLIOGRAPHY

1. Moore, F. K. and Maslen, S. H., "Transverse Oscillations in a Cylindrical Combustion Chamber," NACA TN 3152, October 1954.

2. Crocco, L., Grey, J., and Harrje, D. T., "Theory of Liquid Propellant Rocket Combustion Instability and Its Experimental Verification," ARS Journal, February 1960.

3. Osborn, J. R. and Bonnell, J. M., "An Experimental Investigation of Traverse Mode Combustion Oscillations in Premixed Gaseous Bipropellant Rocket Motors," Purdue University Report No. I-60-1, January 1960.

4. Bonnell, J. M., "An Experimental Investigation of Transverse Mode Combustion Oscillations in Premixed Gaseous Bipropellant Rocket Motors," M.S. Thesis, Purdue University, January 1960.

5. Osborn, J. R. and Schiewe, R. M., "An Experimental Investigation of High Frequency Combustion Pressure Oscillations in a Gaseous Bipropellant Rocket Motor," Purdue University Report No. I-58-1, June 1958.

6. Schiewe, R. M., "An Experimental Investigation of High Frequency Combustion Pressure Oscillations in a Gaseous Propellant Rocket Motor," M.S. Thesis, Purdue University, June 1959.

7. Osborn, J. R. and Pinchak, A. C., "Investigation of Aerothermodynamic Interaction Phenomena in Combustion Pressure Oscillations," Purdue University Report No. I-59-2, June 1959.

8. Pinchak, A. C., Investigation of Aerothermodynamic Interaction Phenomena in Combustion Pressure Oscillations," M.S. Thesis, Purdue University, June 1959.

9. Osborn, J. R., "An Experimental Study of Combustion Pressure Oscillations in a Gaseous Bipropellant Rocket Motor," Ph.D. Thesis, Purdue University, June 1957.

10. Markstein, G. H., and Schwartz, P., "Interaction Between Pressure Waves and Flame Fronts," Jet Propulsion, April 1955.

11. Morse, P. M., Vibration and Sound, McGraw-Hill Book Company, Inc., 1948, pp. 183-191, 397-399.

12. Wylie, C. R, Jr., Advanced Engineering Mathematics, McGraw-Hill Book Company, Inc., 1951, pp. 249-288.

13. Maslen, S. H., and Moore, F. K., "On Strong Transverse Waves Without Shocks in a Circular Cylinder," Journal of Aeronautical Science, Vol. 23, No. 6, 1955.

14. Mickelson, W. R., "Effect of Standing Transverse Acoustic Oscillations on Fuel-Oxidant Mixing in Cylindrical Combustion Chambers," NACA TN 3983, May 1957.

APPENDICES

APPENDIX A

NOTATION

a - velocity of sound

A_o - area of orifice

c_p - specific heat at constant pressure

c_v - specific heat at constant volume

cps. - cycles per second

D - inside diameter of combustion chamber

d.c. - direct current

EyA - ethylene-air propellant combination

E.R. - equivalence ratio

f - oscillation frequency

g - local acceleration due to gravity

J_m - Bessel function of order m

k - specific heat ratio (c_p/c_v)

K_o - orifice flow coefficient

L - length of combustion chamber

p - mean static pressure

p' - instantaneous static pressure

P_c - mean combustion chamber pressure

psi - pounds per square inch

psia - pounds per square inch, absolute

psig - pounds per square inch, gage

psid - pounds per square inch, differential

R - radius

R_g - gas constant

R - degrees Rankine

sec. - second

t - time

T - absolute temperature

$\bar{v}$ - instantaneous particle velocity

$\dot{w}$ - weight rate of flow

Y - expansion factor

γ - specific weight

ρ - density of a given medium

Δp - static pressure drop across an orifice

ω_r - oscillation frequency in radial plane

ω_z - oscillation frequency in axial plane

APPENDIX B

THEORETICAL ACOUSTIC OSCILLATIONS

The classical acoustic wave equation,

$$a^2 \nabla^2 p' = \frac{\partial^2 p'}{\partial t^2} \tag{1}$$

is limited to weak amplitude oscillations, no heat addition, and no mass flow in or out of the resonant column. Combustion pressure oscillations in rocket motors occur having high amplitude fluctuations, heat addition, and mass flow in and out of the chamber. It, therefore, seems questionable to use this equation as a theoretical approach to the problem. It has been found, however, that the frequency of oscillations are surprisingly well described by classical acoustics. It seems justifiable, then, to consider the solution of the wave equation as a guide to oscillation frequencies in rocket motor combustion chambers.

The wave equation expressed in cylindrical coordinates (r, θ, z) is:

$$\frac{\partial^2 p'}{\partial t^2} = a^2 \left(\frac{\partial^2 p'}{\partial Z^2} + \frac{\partial^2 p'}{\partial r^2} + \frac{1}{r}\frac{\partial p'}{\partial r} + \frac{1}{r^2}\frac{\partial^2 p'}{\partial \theta^2}\right) \tag{2}$$

The general solution* to this equation as given in Reference (11) is:

$$p' = \begin{matrix}\cos \\ \sin\end{matrix} (m\theta) \cos \left(\frac{\omega_z Z}{a}\right) J_m \left(\frac{\omega_r r}{a}\right) e^{-i2\pi ft} \tag{3}$$

---

* A discussion of the method of solving equations of this type is given in Reference (12).

where:

$$\omega_z = \frac{\pi \eta_z a}{L} \qquad (\eta_z = 0, 1, 2, 3....) \tag{4}$$

$$\omega_r = \frac{\pi \alpha_{mn} a}{R} \tag{5}$$

$$f = \frac{a}{2}\sqrt{\left(\frac{\eta_z}{L}\right)^2 + \left(\frac{\alpha_{mn}}{R}\right)^2} \tag{6}$$

Where η_z, m, n are wave numbers for the axial (longitudinal), tangential, and radial modes respectively. If only one of the wave numbers is not zero, the mode is said to be "pure." If more than one is not zero, the corresponding mode is a "combination" mode. There are an unlimited number of combinations depending on the values of η_z, m, and n.

The quantities α_{mn} are roots of the equation $dJm(\pi\alpha)/d\alpha = 0$ which is required in the solution of the wave equation. Some selected values of α_{mn} as given in Reference (11) are as follows:

m \ n	0	1	2	3
0	0.000	1.2197	2.2331	3.2383
1	0.5861	1.6970	2.7140	3.7261
2	0.9722	2.1346	3.1734	4.1923
3	1.13373	2.5513	3.6115	4.6428

Pressure Fluctuations

For a "pure" first tangential mode, m = 1, n = η_z = 0. The corresponding pressure function is:

$$p' = J_1\left(\frac{2\pi f r}{a}\right) \cos\theta \; e^{-i2\pi f t} \tag{7}$$

where:

$$f = \frac{\alpha_{1,0} a}{2R} \tag{8}$$

Equation (7) may be written:

$$p' = J_1 \left(\frac{2\pi fr}{a}\right) \cos\theta \left[\cos(2\pi ft) - i \sin(2\pi ft)\right] \tag{9}$$

Using the real part:

$$p' = J_1 \left(\frac{2\pi fr}{a}\right) \cos\theta \cos(2\pi ft) \tag{10}$$

For a "pure" first radial mode, $n = 1$, $m = \eta_z = 0$.

The corresponding pressure function is:

$$p' = J_0 \left(\frac{2\pi fr}{a}\right) e^{-i 2\pi ft} \tag{11}$$

where in this case:

$$f = \frac{\alpha_{0,1} a}{2R} \tag{12}$$

Using the real part of equation (11):

$$p' = J_0 \left(\frac{2\pi fr}{a}\right) \cos(2\pi ft) \tag{13}$$

Expressions for the pressure fluctuations for other modes can be found by using different values of m, n, and η_z.

Particle Velocity

A relationship for the particle velocity as a function of the pressure fluctuation can be obtained from Newton's equation of motion:

$$\rho \left(\frac{\partial \bar{v}}{\partial t}\right) = - \nabla p' \tag{14}$$

Substituting into equation (14) for p' from equation (3) we get

$$\rho \left(\frac{\partial \bar{v}}{\partial t}\right) = - \nabla \left[\cos (m\theta) \cos \left(\frac{\omega_z Z}{a}\right) J_m \left(\frac{\omega_r r}{a}\right) e^{-i2\pi ft}\right] \qquad (15)$$

Rearranging and integrating both sides:

$$\bar{v} = \frac{1}{i\rho 2\pi f} \nabla \left[\cos (m\theta) \cos \left(\frac{\omega_z Z}{a}\right) J_m \left(\frac{\omega_r r}{a}\right) e^{-i2\pi ft}\right] \qquad (16)$$

The equation of the particle velocity as a function of the pressure fluctuations (from equation (16)) is:

$$\bar{v} = \frac{1}{i\rho 2\pi f} \nabla p' \qquad (17)$$

The equations derived in this report serve to give a physical picture of the oscillations found in cylindrical combustion chambers. Figure 25* represents the pressure and particle velocity for some selected modes. It can be noted from Fig. 25 that a "spinning" mode is the same as a standing tangential mode except the "spinning mode spins within the chamber whereas the standing tangential mode sloshes back and forth in the chamber. The frequencies of the two, however, are the same. A more detailed discussion of traveling waves is given in Reference (13). Complete solutions of the above equations are given in References (1), (13), and (14).

Oscillation Frequencies

The theoretical frequencies of the pressure oscillations are given by equation (6). The speed of sound was calculated, assuming a perfect

---

* Figure 25 is a correction of Fig. 25 in Purdue University Report I-60-1.

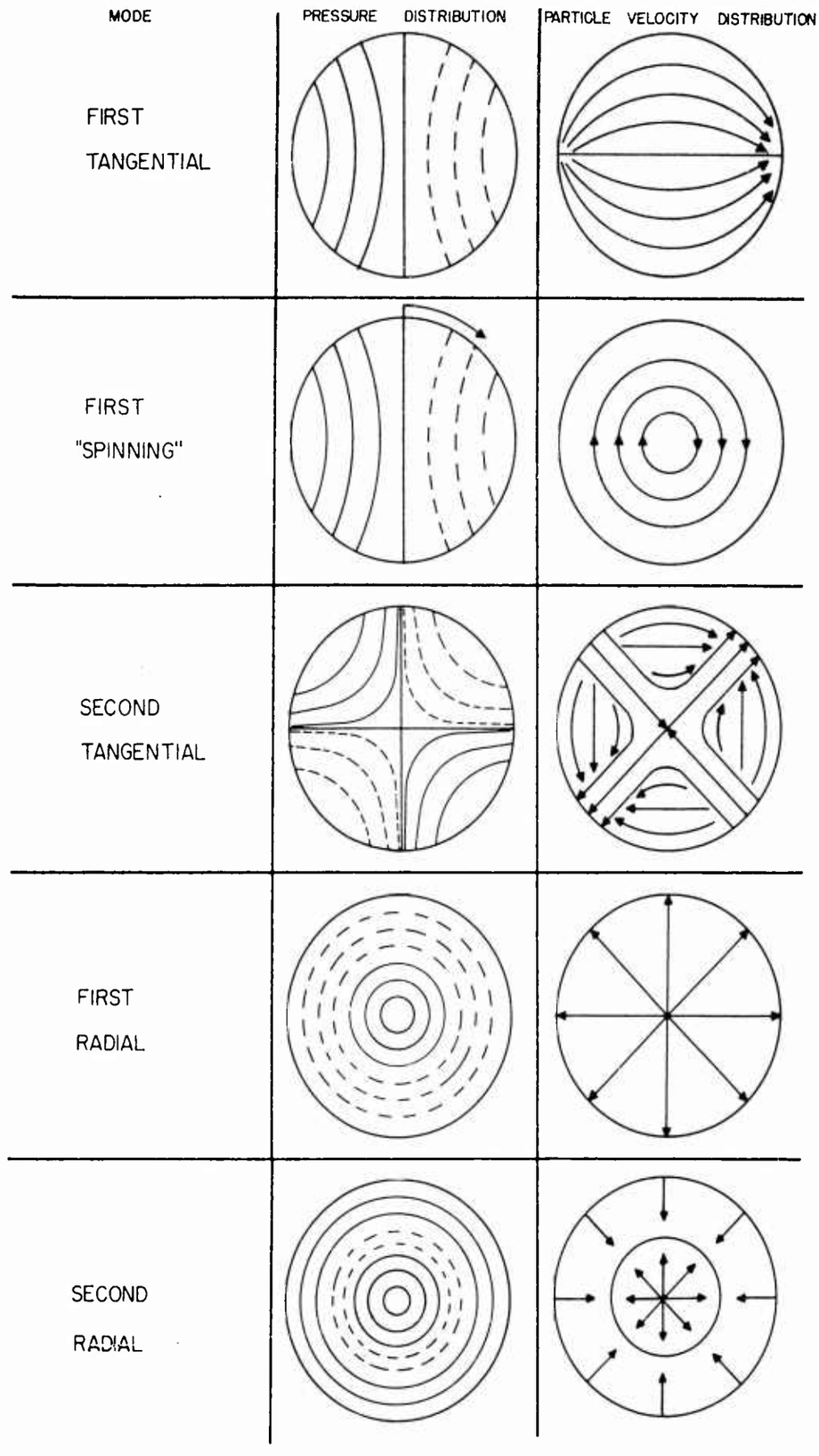

Fig. Theoretical Transverse Modes

gas, from the equation

$$a = \sqrt{kg\ R_g T} \tag{18}$$

For an equivalence ratio of 1.0 the adiabatic flame temperature for ethylene and air is 4200°R. The speed of sound at this temperature is:

$$a = \left[(32.2)(1.27)(53.6)(4200) \right]^{1/2} = 3028 \text{ fps}$$

Since the diameter of the combustion chamber used in this investigation was 7 in., 2 R is 0.582 ft.

For a first radial mode, $\alpha_{mn} = 1.2197$. The theoretical frequency of the first radial mode is:

$$f = \frac{(1.2197)(3028)}{0.582} = 6300 \text{ cps}$$

For the first tangential or "spinning" mode $\alpha_{mn} = 0.5861$. The corresponding frequency is:

$$f = \frac{(0.586)(3028)}{0.582} = 3200 \text{ cps}$$

The frequencies of the second radial and tangential modes can be calculated using α_{mn} equal to 2.2381 and 0.9722 respectively.

Since the speed of sound in the combustion chamber is a function of the flame temperature; the frequency of the oscillations decreases as the propellant mixture ratio is increased or decreased from stoichiometric (8).

APPENDIX C

DESCRIPTION OF APPARATUS

Test Cell and Control Room

Figure 26 illustrates the plan view of the test cell and control room in which the rocket motor under investigation, propellant feed lines, and control components were mounted. The rocket motor was controlled remotely from the control room. The steady state and high frequency instrumentation was also located in the control room.

Research Rocket Motor

A 7 in. diameter premixed gaseous propellant rocket motor was used in all three phases of this investigation. The only parameters that were varied were injection location, chamber length, mean chamber pressure, and equivalence ratio. All other parameters were held constant.

Figure 27 is a cross section of the motor used for the head end injection studies. Figure 28 is a cross section of the injection scheme used in this phase. The fuel and oxidizer were mixed in the mixing chamber. After mixing, the propellants passed through "sonic holes" to the injector. These holes were designed to isolate the combustion chamber from the feed lines. This prevented low frequency oscillations in the chamber (chugging phenomenon) and flash-back* into the mixing chamber.

---

* Burning in the mixing chamber.

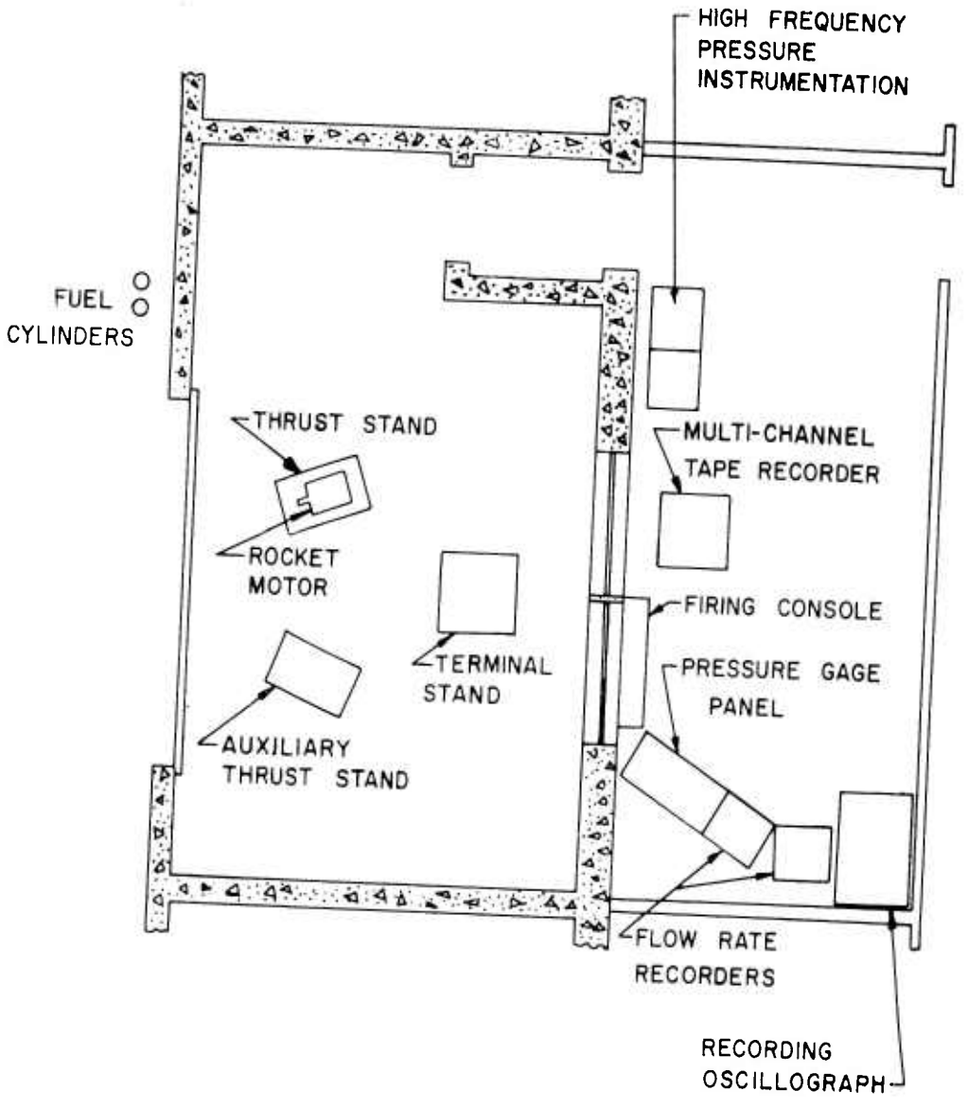

Fig. 2 Test Cell Arrangement

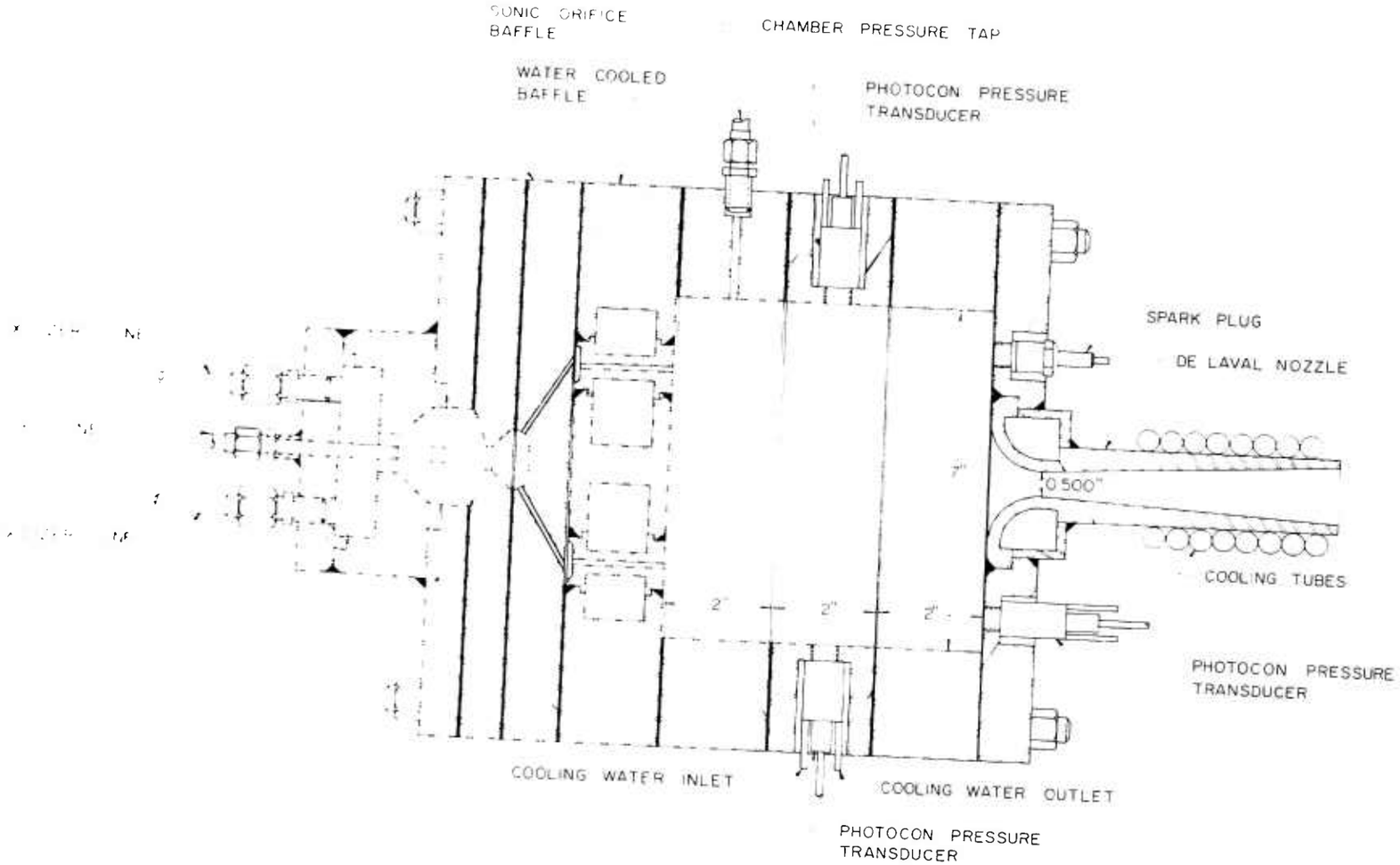

Fig. 27 Sectional View of the Rocket Motor

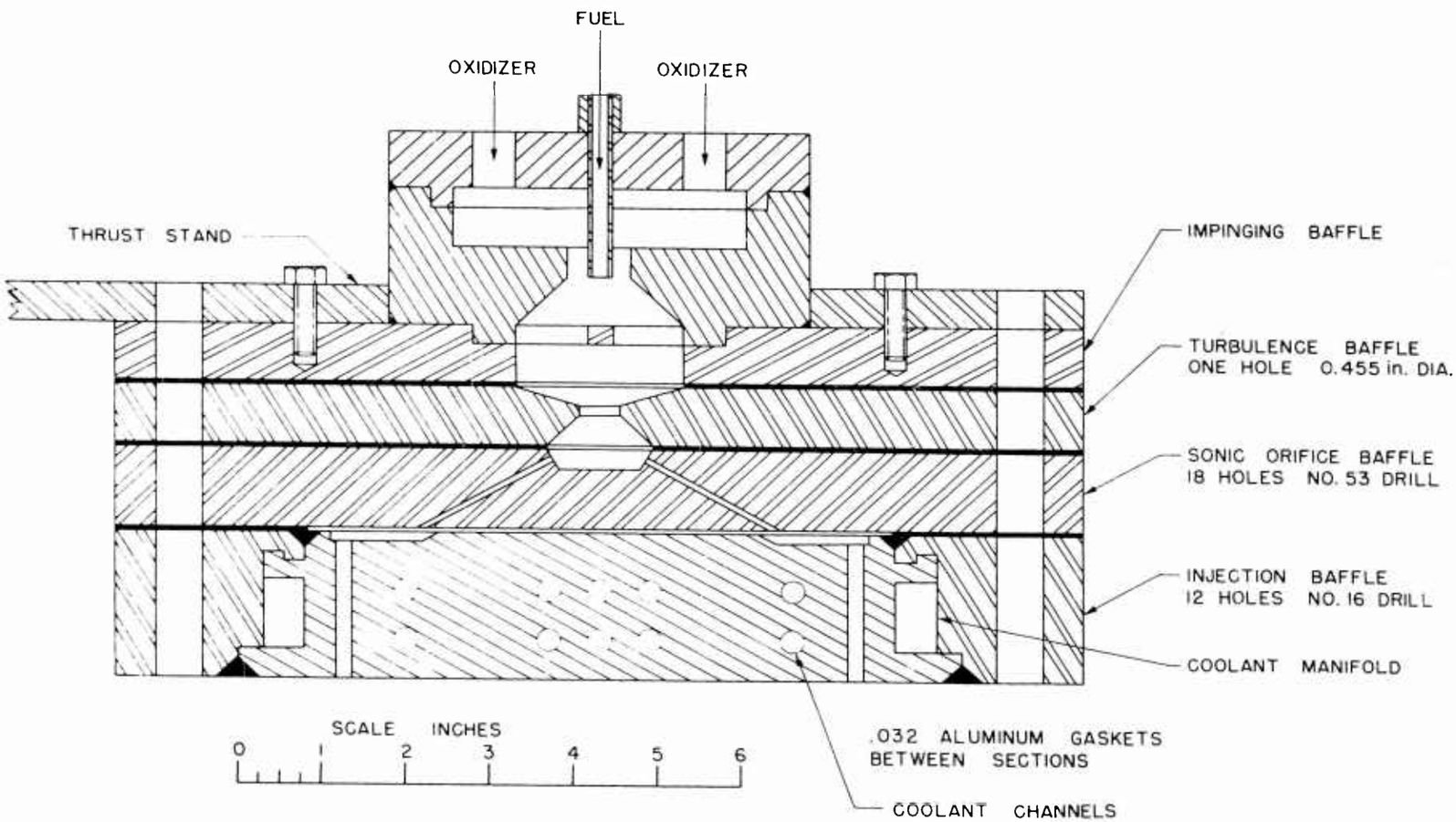

Fig. 28 Sectional View of the Head End Injector

After passing through the "sonic orifice baffle," the propellants passed through a water cooled injector to the chamber. The injection holes (in all cases 0.177 in. in diameter) in the injector plate were arranged in three different patterns. The three injection patterns are presented in Fig. 3.

Figure 29 is a cross section of the motor used in the side injection studies. The mixing chamber was external to the motor and the mixed propellants were transmitted to the different injector units through tubes. Six individual injector units were equally spaced around a 2 in. long combustion chamber spacer. A photograph of the motor with side injection is presented in Fig. 2.

Figure 30 is a cross section of an injector unit. The injector unit consisted of an injection baffle and a sonic orifice baffle fitted together. These parts were made of stainless steel since the injector units were uncooled.

In the nozzle end injection motor, the afore-mentioned injector units were placed in tapped holes in the nozzle plate. They were arranged so that the injection pattern was identical to that of the head end injector with the injection holes on a 6 in. injection circle diameter (see Fig. 3 injector A).

The nozzle used in all the motors in this investigation was a DeLaval nozzle with a 0.50 in. throat diameter. The converging-diverging part of the nozzle was made of stainless steel, while the flange part of the nozzle was made of mild steel. A water cooling jacket cooled the converging approach and throat, while external cooling tubes cooled the diverging section of the nozzle. Since thrust was of no interest in this

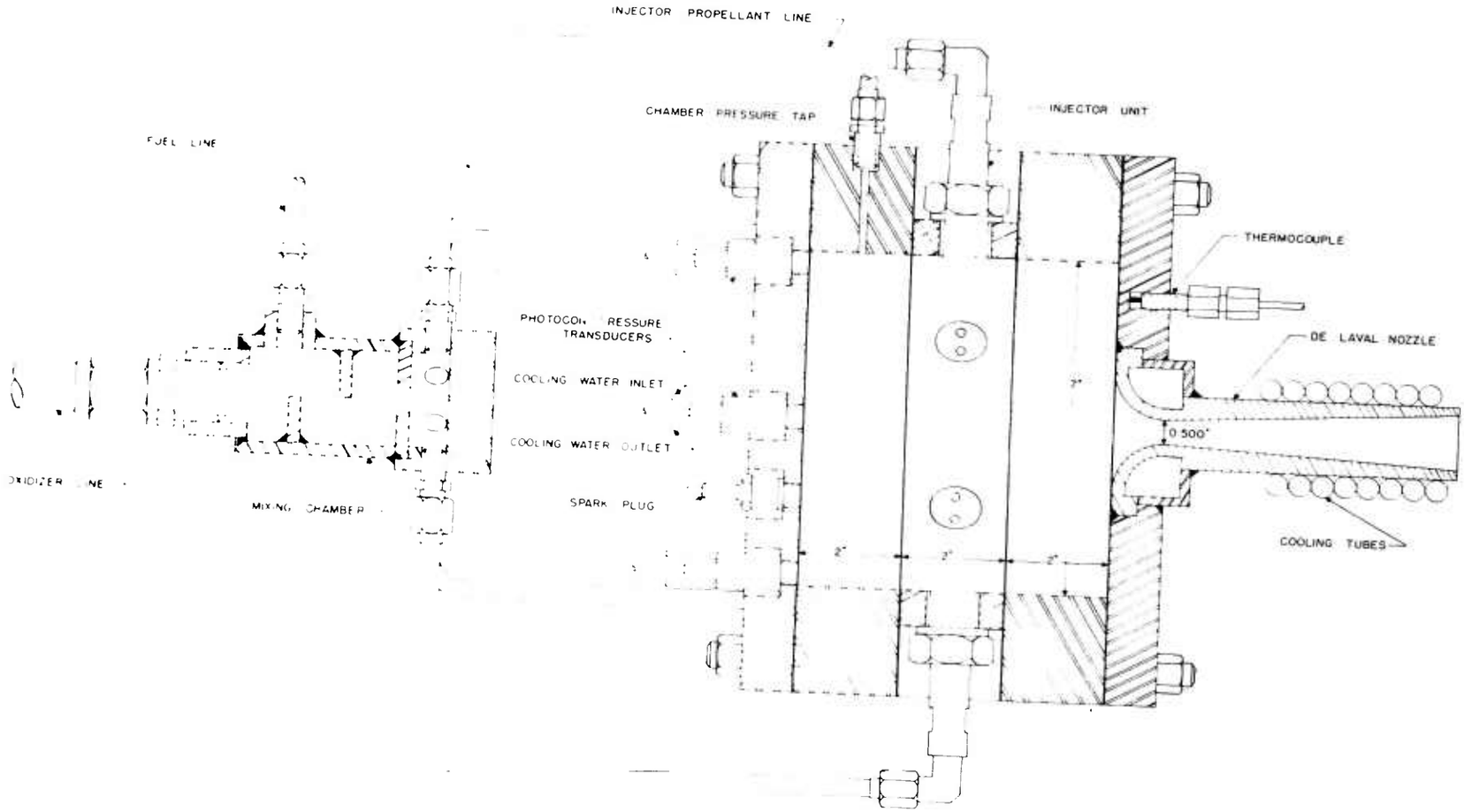

Fig. 29 Sectional View of the Rocket Motor

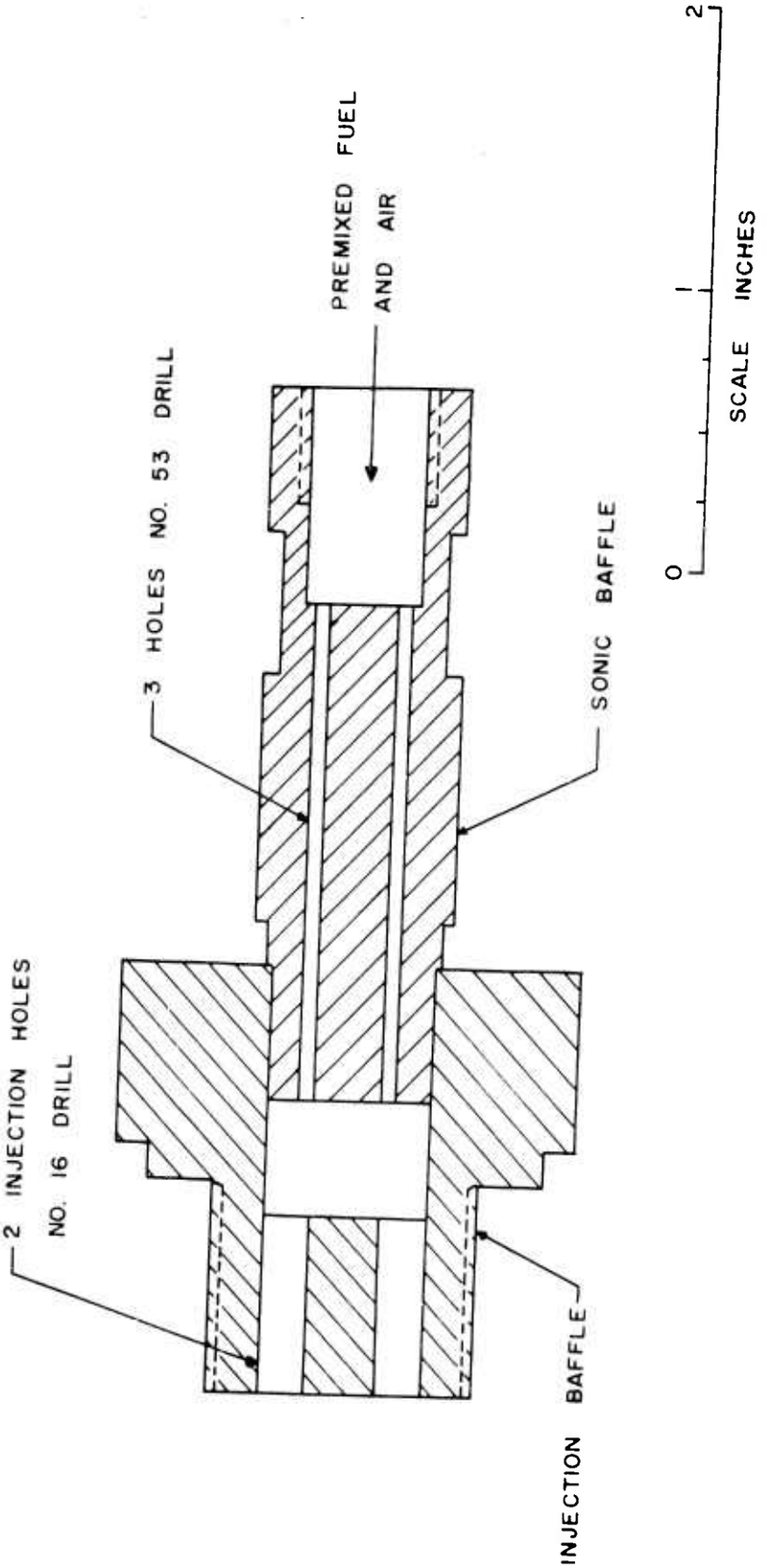

Fig. 30 Individual Injector Unit

investigation, the diverging section of the nozzle was employed for protecting the instrumentation mounted in the nozzle plate from the hot exhaust gases.

Tapped holes were provided in the chamber sections, head plate, and nozzle plate for mounting igniter plugs, pressure transducers, thermocouples, pressure taps, and other auxiliary fittings.

An ordinary automotive spark plug was used to ignite the propellants in the chamber. The spark plug was energized by an aircraft engine magneto (Allison V 1710). The magneto was driven by a 1/4 horsepower electric motor.

Propellant Supply System

The propellants used in this investigation were gaseous ethylene and air. Figure 31 is a schematic diagram of the plumbing system used to control and supply the propellants to the motor. The fuel was supplied from commercial compressed gas cylinders. A bank of two or more of these cylinders were connected to the fuel supply line through a manifold. The initial supply pressure was about 1200 psig.

The fuel flow was controlled by hand valves on the cylinders, a solenoid operated shut-off valve, and an externally controlled Grove pressure regulator (Type RBX 204-015). The Grove regulator controlled the upstream pressure to a sharp edge, thin plate metering orifice. This regulated the fuel flow rate through the orifice. The control air in the Grove regulator was varied by a hand operated Atlas pressure regulator in the control room. After passing through the metering orifice, the fuel flowed to a bipropellant valve (obtained from an Aerojet 38 ALDW-1500 JATO unit) and thence to the motor.

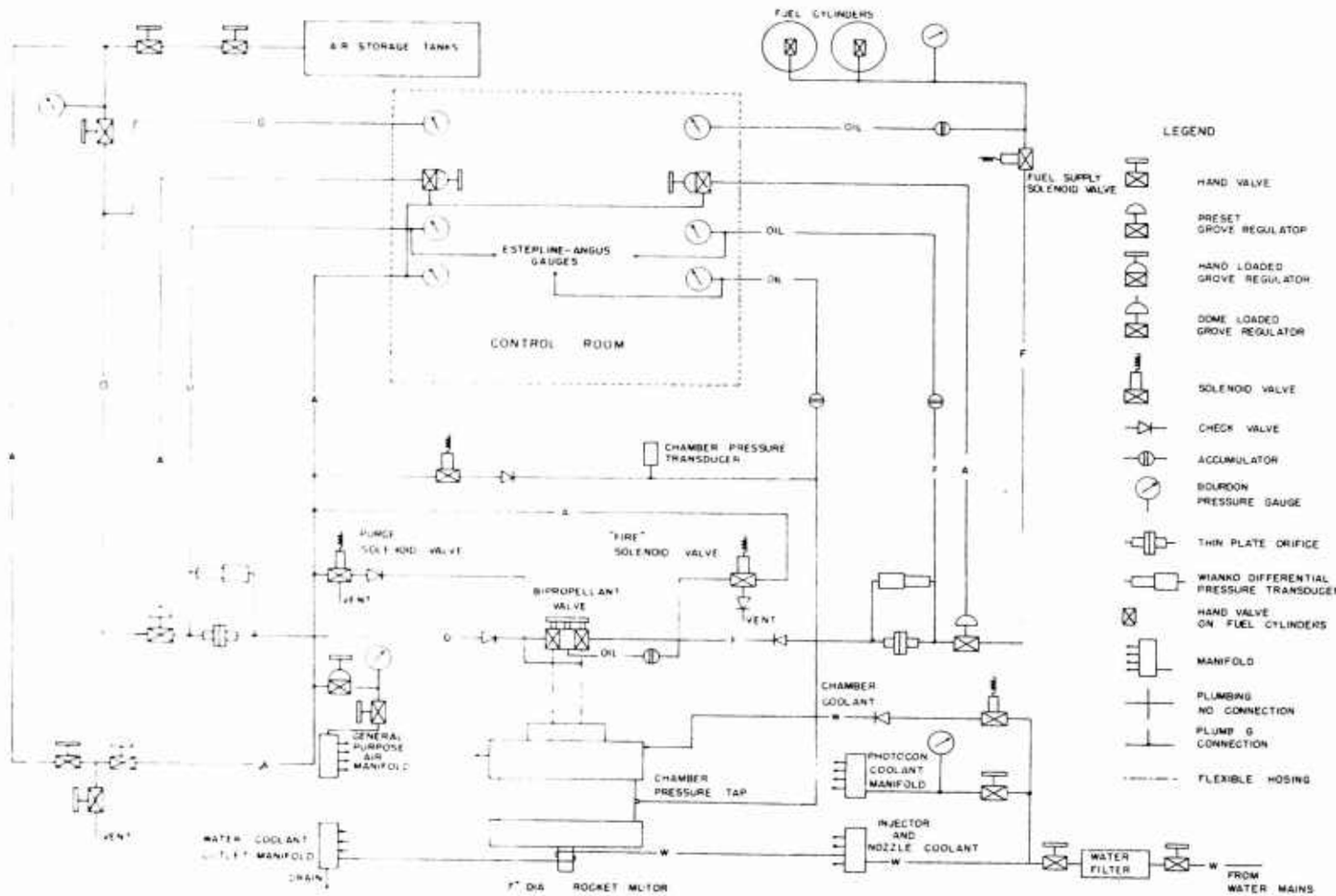

Fig. 31 Piping System

Air was supplied to the system from a bank of pressure tanks at a pressure of about 1500 psig. The air in these tanks was replenished when needed from a centrally located compressor at the Jet Propulsion Center.

After the air passed through a series of hand valves, it passed through an externally controlled Grove regulator (Type WBX 306-04). The regulator was controlled by air from an Atlas pressure regulator in the control room. Downstream from the Grove regulator was a sharp edged, thin plate metering orifice. The air flow rate was controlled by varying the upstream pressure to the orifice with the Grove regulator. After passing through the orifice, the air flowed to the bipropellant valve and thence to the motor.

Instrumentation

Steady State Instrumentation

Figure 32 is a photograph of the steady state instrumentation in the control room. The steady state parameters indicated in this investigation were propellant temperatures, orifice pressure drops, pressures upstream to the orifices, fuel and air supply pressures, Grove regulator control pressures, combustion chamber wall temperature, and mean combustion pressure.

The thin plate orifices were used for metering the flow of fuel and air. The pressure drop across the orifices was measured by Wiancko differential pressure transducers (Model P 1203). The signals from the transducers were recorded on two Minneapolis-Honeywell (Model 153x18-V-II-III-118-N2) self-balancing potentiometer recorders.

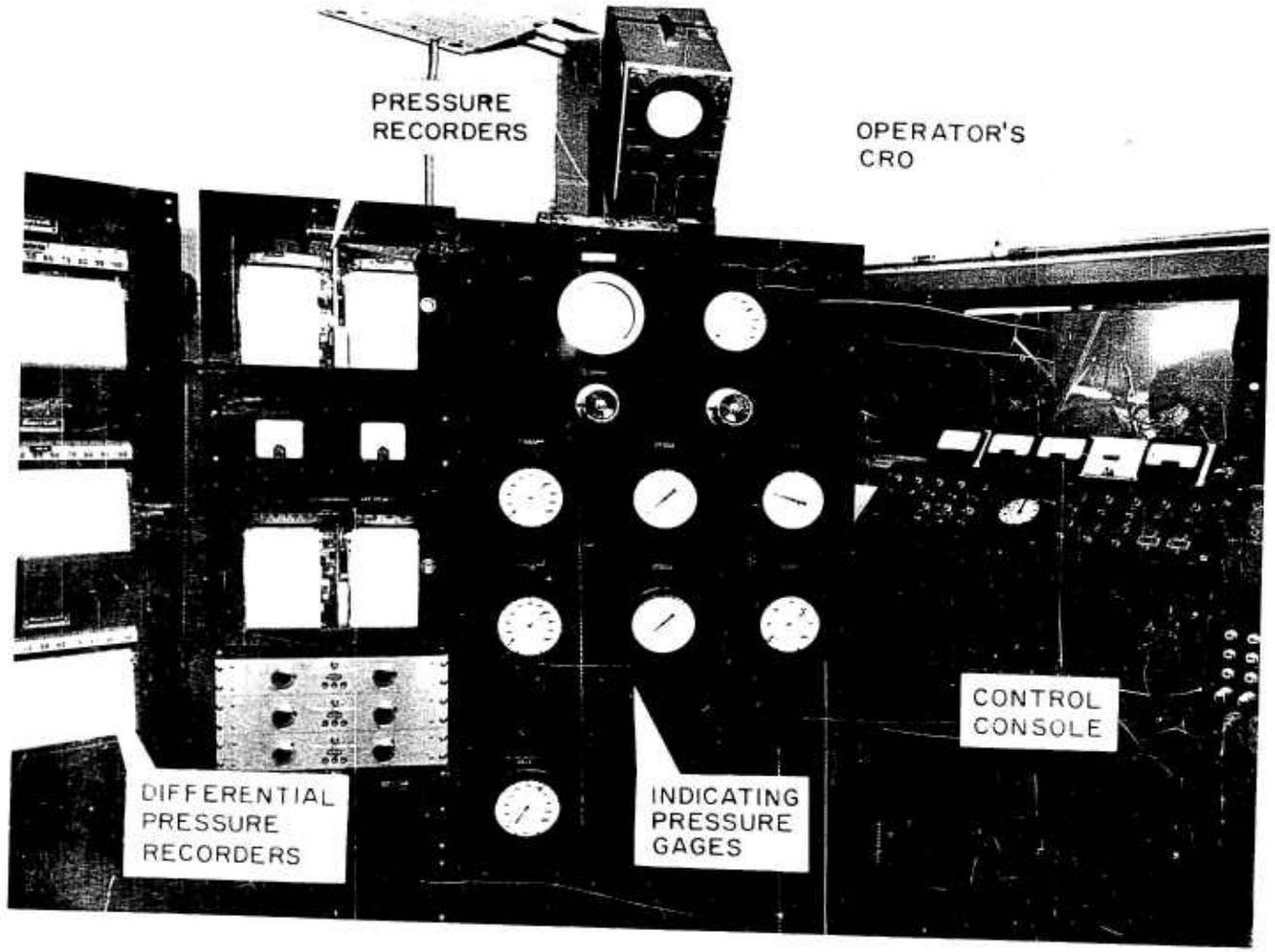

Fig. 32 Static Instrumentation

Conventional iron-constantan thermocouples were used to measure all temperatures. Simplytrol millivoltmeters were used to indicate the temperatures to the operator. The propellant temperatures were used in the calculation of the propellant densities.

The pressures upstream to the two orifices and the combustion chamber pressure were recorded on Esterline Angus Bourdon type pressure recorders. Bourdon type pressure gages were used to indicate all static pressures.

High Frequency Instrumentation

Figure 33 is a photograph of the high frequency instrumentation in the control room. The pressure oscillations in the combustion chamber were measured with flush mounted Photocon* (Models 342 and 343) pressure transducers. Dynagage units (Model D.G. 400 or D.G. 101 and power supply) were used to convert the signals from the transducers to a voltage output that was proportional to the pressure in the combustion chamber.

The signals from the Dynagage units were recorded on an Ampex Series FR-100B multi-channel tape recorder/reproducer. The reproduced signals from the tape recorder were recorded for visual observation by using a Hathaway model SC-16 B six-channel recording oscillograph.

A Dumont type 304-H cathode ray oscilloscope and a Tetronix type 502 dual beam cathode ray oscilloscope were used to monitor the pressure oscillation signals from the Ampex tape recorder or Dynagage units.

---

* A discussion of the frequency and transient response characteristics of Photocon transducers and associated equipment is given in Reference (9).

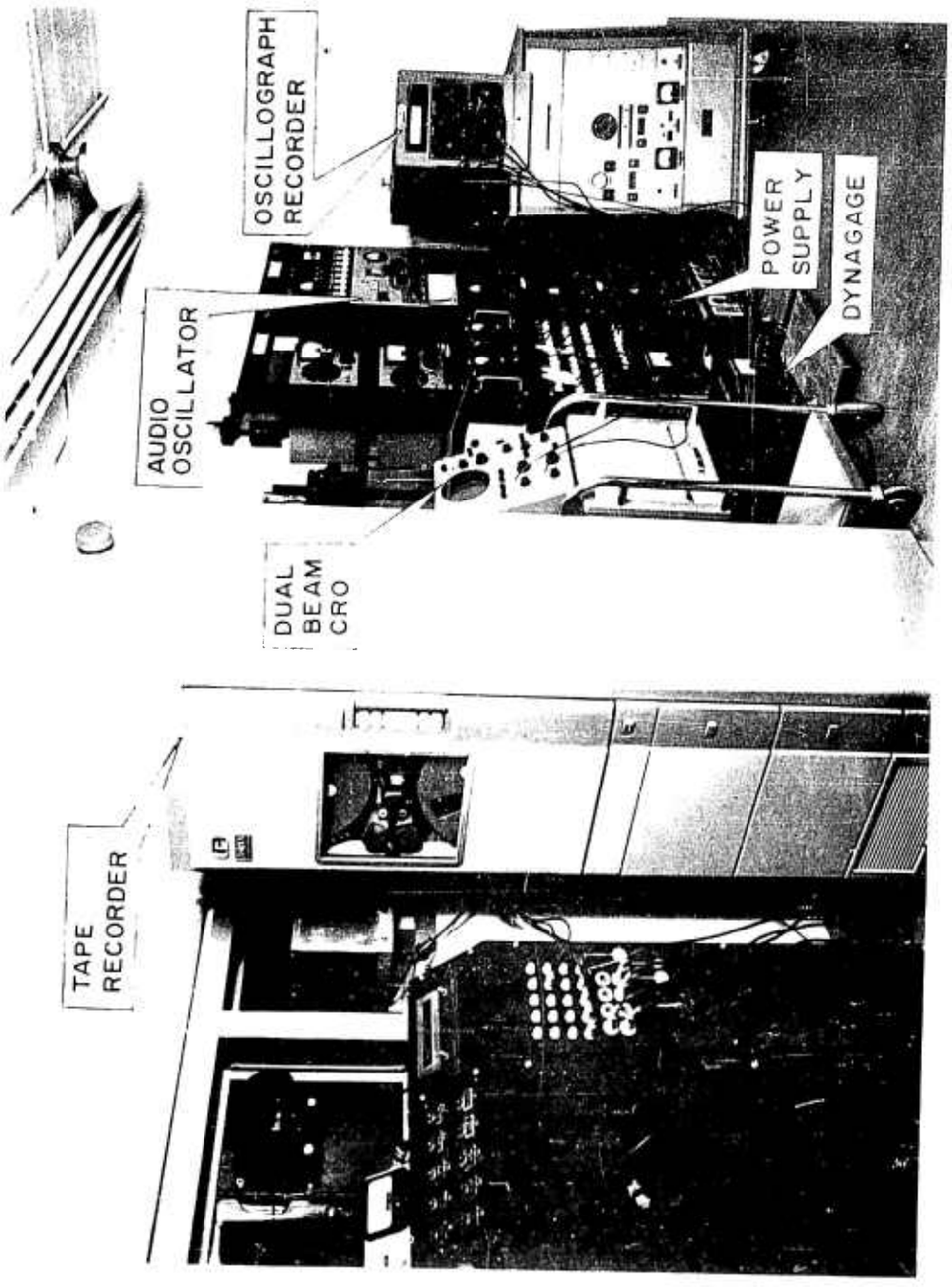

Fig. 33 Dynamic Instrumentation

APPENDIX D

PROCEDURE FOR CONDUCTING A ROCKET MOTOR RUN AND EVALUATING THE DATA

Calibration of Equipment

Steady State Measuring Equipment

Before each test run was initiated, all necessary equipment was calibrated. The Bourdon type pressure gages were only checked periodically due to their high reliability. The electrical differential pressure transducers, however, were calibrated prior to each run with an Ashcroft Gage Tester, Type 1300. The thermocouples used to measure the various temperatures were calibrated only at the time of their installation and were checked periodically for accuracy.

High Frequency Measuring Equipment

Since the output from each Photocon-Dynagage combination was different, it was necessary to calibrate each Photocon with the Dynagage unit it was being used with during the run. They were calibrated statically every two weeks or 30 days depending on the frequency of use. Calibration consisted of applying a known pressure to the Photocon with compressed air and measuring the voltage output from the Dynagage. Since the output from the Dynagage units was linear with pressure, it was only necessary to take two readings. The result was a constant (psi/volt)

relating the pressure applied to the Photocon to the voltage output of the Dynagage.

The Ampex record and reproduce units were checked and adjusted periodically according to the "Performance Check" instructions in the Ampex manual.

Firing the Rocket Motor

After combustion was initiated in the rocket motor, a desired operating condition was obtained by adjusting the flow rates of the propellants. At the desired chamber pressure and equivalence ratio the steady state recording instruments were marked and the point was correlated with the pressure recordings on the tape recorder by means of the audio channel of the tape recorder. The procedure was repeated for other desired operating conditions. When the chamber walls had reached approximately 800°F, the run was terminated. The motor was cooled after each run by forcing water into the chamber and out drain holes. The water was purged from the chamber before another run was initiated. This procedure was repeated until sufficient data were obtained to define the instability region and oscillation amplitudes for the motor under investigation.

Evaluating the Data

The Ampex tape recorder used in this investigation had a tape transport which could be operated at six different rotational speeds. This made it possible to record at one speed and reproduce at another. Recordings of the high frequency oscillations were made at a tape speed of 60 in./sec and were reproduced at a speed of 1 7/8 in./sec. The time base change was 32:1. This made it possible to record much higher

frequencies on the Hathaway oscillograph recorder than was possible without the tape recorder.

The amplitude of the pressure oscillations was determined by comparing the Hathaway record of the taped pressure signals to a prerecorded taped calibration signal. This was then compared to the calibration of the Photocon-Dynagage combination described above.

The propellant flow rates were calculated from the equation

$$\dot{w} = 0.668\, K_o A_o Y_o \sqrt{\gamma \Delta p} \qquad (19)$$

where Δp is the metering orifice pressure drop and γ is the specific weight of the propellant upstream to the orifice. The propellant was assumed to obey the perfect gas law. The specific weight could therefore be calculated from the formula:

$$\gamma = \frac{p}{RT} \qquad (20)$$

The equivalence ratio for each data point was found by dividing the rate of fuel flow by the rate of air flow and dividing the result by the stoichiometric fuel-air ratio by weight for the propellant combination.

"Distribution of this report has been made in accordance with the Joint Army-Navy-Air Force Liquid Propellant Mailing List of November 1960."